

Some remarks on the spectral functions of the Abelian Higgs model

D. Dudal,^{1,2,*} D. M. van Egmond,^{3,†} M. S. Guimarães,^{3,‡} O. Holanda,^{3,§} B. W. Mintz,^{3,||} L. F. Palhares,^{3,¶}
G. Peruzzo,^{3,**} and S. P. Sorella^{3,††}

¹*KU Leuven Campus Kortrijk-Kulak, Department of Physics,
Etienne Sabbelaan 53 bus 7657, 8500 Kortrijk, Belgium*

²*Ghent University, Department of Physics and Astronomy, Krijgslaan 281-S9, 9000 Gent, Belgium*

³*Universidade do Estado do Rio de Janeiro, Instituto de Física-Departamento de Física Teórica-Rua São Francisco Xavier 524, 20550-013 Maracanã, Rio de Janeiro, Brasil*



(Received 31 May 2019; published 16 September 2019)

We consider the unitary Abelian Higgs model and investigate its spectral functions at one-loop order. This analysis allows us to disentangle what is physical and what is not at the level of the elementary particle propagators, in conjunction with the Nielsen identities. We highlight the role of the tadpole graphs and the gauge choices to get sensible results. We also introduce an Abelian Curci-Ferrari action coupled to a scalar field to model a massive photon which, like the non-Abelian Curci-Ferrari model, is left invariant by a modified non-nilpotent BRST symmetry. We clearly illustrate its nonunitary nature directly from the spectral function viewpoint. This provides a functional analogue of the Ojima observation in the canonical formalism: there are ghost states with nonzero norm in the BRST-invariant states of the Curci-Ferrari model.

DOI: [10.1103/PhysRevD.100.065009](https://doi.org/10.1103/PhysRevD.100.065009)

I. INTRODUCTION

In recent years there has been an increasing interest in the properties of the spectral function (Källén-Lehmann density) of two-point correlation functions, especially in non-Abelian gauge theories such as quantum chromodynamics (QCD). It was found [1–5], in lattice simulations for the minimal Landau gauge, that the spectral function of the gluon propagator is not non-negative everywhere, which means that there is no physical interpretation for this propagator like there is for the photon propagator in quantum electrodynamics (QED). This behavior of the gluon spectral function is commonly associated with the concept of confinement [6–9]. The nonpositivity of the spectral function then becomes a reflection of the inability of the gluon to exist as a free physical particle, i.e., as an observable asymptotic state of the S -matrix.

Many properties of the nonperturbative infrared region of QCD are coherently described today by lattice simulations [10]. Analytically, however, despite the progress made in the last decades, the achievement of a satisfactory understanding of the infrared (IR) region is still a big challenge. The gluon propagator is not gauge invariant, and therefore one needs to fix a gauge using the Faddeev-Popov (FP) procedure, introducing ghost fields, while trading the local gauge invariance with the Becchi-Rouet-Stora-Tyutin (BRST) symmetry. In the perturbative ultraviolet region of QCD, the FP gauge fixing procedure works, giving results in excellent agreement with experiments. However, an extrapolation of the perturbative results to low energies is plagued by infrared divergencies caused by the existence of the well-known Landau pole. In the same region, it is known that the standard FP procedure does not fix the gauge uniquely: several field configurations satisfy the same gauge condition, e.g., the transverse Landau gauge, leading to the so-called Gribov copies [11,12]. Over the years, various attempts have been made to deal with this problem in the continuum functional approach; see for example [13–18].

The problem of the Landau pole in asymptotically free theories can be provisionally circumvented, with an adequate renormalization scheme, by the introduction of an effective infrared gluon mass [19]. This is in accordance with the lattice data, which show that the gluon propagator reaches a finite positive value in the deep IR for space-time Euclidean dimensions $d > 2$; see e.g., [20–28]. Of course, analytically one would like to recover the massless

* david.dudal@kuleuven.be
† duifjefmaria@gmail.com
‡ msguimaraes@uerj.br
§ ozorio.neto@uerj.br
|| bruno.mintz@uerj.br
¶ leticia.palhares@uerj.br
** gperuzzofisica@gmail.com
†† silvio.sorella@gmail.com

Published by the American Physical Society under the terms of the [Creative Commons Attribution 4.0 International license](https://creativecommons.org/licenses/by/4.0/). Further distribution of this work must maintain attribution to the author(s) and the published article's title, journal citation, and DOI. Funded by SCOAP³.

character of the FP gauge fixing theory in the perturbative UV region. The use of such theory which implements an effective mass only in the IR region was first proposed in [29] based on the idea of a momentum-dependent or dynamical gluon mass [30,31]. For this, the Schwinger-Dyson equations are employed in order to get a suitable gap equation that governs the evolution of the dynamical gluon mass $m(p^2)$, which vanishes for $p^2 \rightarrow \infty$. This setup preserves both renormalizability and gauge invariance. However, the Schwinger-Dyson equations are an infinite set of coupled equations which require a truncation procedure; see for example [32–36] for a detailed presentation of the subject.

Recently, a more pragmatic approach was taken in [16,37,38], or in other works like [39–41]. Instead of a model justified from first principles, the observations obtained from lattice simulations were used as a guiding principle. The massive gluon propagators observed in lattice simulations for Yang-Mills theories led to considering the following action:

$$S = \int d^d x \left\{ \frac{1}{4} F_{\mu\nu}^a F_{\mu\nu}^a + \bar{c}^a \partial_\mu (D_\mu c)^a + i b^a \partial_\mu A_\mu^a + \frac{m^2}{2} A_\mu^a A_\mu^a \right\}, \quad (1)$$

which is a Landau gauge FP Euclidean Lagrangian for pure gluodynamics, supplemented with a gluon mass term. This term modifies the theory in the IR but preserves the FP perturbation theory for momenta $p^2 \gg m^2$. The action (1) is a particular case of the Curci-Ferrari (CF) model [42]. The mass term breaks the BRST symmetry of the model, which turns out to still be invariant under a modified BRST symmetry [43],

$$s_m A_\mu^a = -D_\mu^{ab} c^b, \quad (2)$$

$$s_m c^a = \frac{g}{2} f^{abc} c^b c^c, \quad (3)$$

$$s_m \bar{c}^a = i b^a, \quad (4)$$

$$s_m b^a = i m^2 c^a, \quad (5)$$

which is, however, not nilpotent since $s_m^2 \bar{c} \neq 0$.

The legitimacy of the model (1) depends, of course, on how well it accounts for the lattice results. In [19,37,38], it has been shown that, both at one- and two-loop order, the model reproduces quite well the lattice predictions for the gluon and ghost propagator. For other applications of (1), we refer to [44–47]. However, from the Kugo-Ojima criterion [48], it is known that nilpotency of the BRST symmetry is indispensable to formulate suitable conditions for the construction of the states of the BRST-invariant physical (Fock) subspace, providing unitarity of the S -matrix. Indeed, in [49,50] the existence of negative norm

states in the s_m -invariant subspace (“the would-be physical subspace”) was confirmed. However, it is worth mentioning here that the goal of [37] and follow-up works was *not* to introduce a theory for massive gauge bosons but to discuss a relatively simple and useful effective description of some nonperturbative aspects of QCD. Unitarity of the gauge bosons sector is not so much an issue, as one expects them to be undetectable anyhow, due to confinement. Within this perspective the existence of an exact nilpotent BRST symmetry becomes a quite relevant property when trying to generalize the action (1) to other gauges than Landau gauge, as next to unitary one should also expect that the correlation functions of gauge-invariant observables are gauge-parameter independent. We will come back to this question in a separate work.

In this context, it is worthwhile to investigate the spectral properties of massive gauge models to try to shed some light on the infrared behavior of their fundamental fields. A direct comparison with a massive model that preserves the original nilpotent BRST symmetry, such as the Higgs-Yang-Mills model, can be particularly enlightening. In any case, the explicit determination of the spectral properties of Higgs theories and the study of the role played by gauge symmetry there are interesting to pursue on their own.

For the $U(1)$ Higgs model, one can fix the gauge by means of ’t Hooft R_ξ -gauge. For the formal limit $\xi \rightarrow \infty$ we end up in the unitary gauge, which is considered the physical gauge as it decouples the nonphysical particles. However, this gauge is known to be nonrenormalizable [51]. Here, we refer the reader to [52] for a recent analysis of the unitary gauge. The Landau gauge, on the other hand, corresponds to $\xi \rightarrow 0$. Most articles on massive Yang-Mills models employ the renormalizable Landau gauge, although it was noticed that this gauge might not be the preferred gauge in nonperturbative calculations [53]. In fact, as was recently established in [54], the use of the Landau gauge in the massive Yang-Mills model (1) leads to complex pole masses, which will obstruct a calculation of the Källén-Lehmann spectral function. Indeed, if at some order in perturbation theory (one loop as in [54] for example) a pair of Euclidean complex pole masses appear, at higher order these poles will generate branch points in the complex p^2 -plane at unwanted locations, i.e., away from the negative real axis, deep into the complex plane, thereby invalidating a Källén-Lehmann spectral representation. This can be appreciated by rewriting the Feynman integrals in terms of Schwinger or Feynman parameters, whose analytic properties can be studied through the Landau equations [55]. Let us also refer to [56,57] for concrete examples.

Understanding the different gauges and their influence on the spectral properties is a delicate subject. This gave us further reason to undertake a systematic study of the spectral properties of Higgs models. In this paper, we present the results for the simplest case: that of the $U(1)$ Abelian Higgs model. In fact, it turned out that this model is

already very illuminating on aspects like positivity of the spectral function, gauge-parameter independence of physical quantities, and unitarity. Of course, these properties are not unknown in the Abelian case. This article should therefore not be seen as giving any new information on the physical properties of the Abelian model. Rather, exactly because these properties are so well known, we are in a better position to understand the problems that we face when calculating the analytic structure behind some of them within a gauge-fixed setup. This work is therefore a first attempt to understand analytically the spectral properties of a Higgs-gauge model in contrast to those of a nonunitary massive model. As such, it is laying the groundwork for future work on these properties in the non-Abelian $SU(2)$ Higgs case as well as in the massive model of [37], Eq. (1), investigating the origin of the complex poles structure reported in [54,58,59].

The $U(1)$ Higgs model is known to be unitary [60,61] and renormalizable [62]. In this work, we consider two propagators: that of the photon and that of the Higgs scalar field. They are obtained through the calculation of the one-loop corrections to the corresponding $1PI$ two-point functions. After adopting the R_ξ -gauge, we are left with an exact BRST nilpotent symmetry. Of course, the correlation function of BRST-invariant quantities should be independent of the gauge parameter. Since the transverse component of the photon propagator is gauge invariant, we should find that the one-loop corrected transverse propagator does not depend on the gauge parameter. As a consequence, neither does the photon pole mass. This property has been proven before by the use of the Nielsen identities, [63] (see also [64–66]) but never in a direct calculation. The same goes for the Higgs particle propagator: the gauge independence of its pole mass was proven in [63] but never in a direct loop calculation, to our knowledge. We underline here the importance of properly taking into account the tadpole contributions [67,68] or, equivalently, the effect on the propagators of quantum corrections of the Higgs vacuum expectation value. Armed with the one-loop results, we are able to calculate the spectral properties of the respective propagators for different values of the gauge parameter. An additional aim of this work is to compare our results with those of a nonunitary massive Abelian model, to clearly pinpoint, at the level of spectral functions, the differences (and issues) of both unitary and nonunitary massive vector boson models.

This article is organized as follows. In Sec. II, we review the $U(1)$ Higgs model and its gauge fixing, as well as the tree-level field propagators and vertices. In Sec. III, we calculate the one-loop propagator of both the photon field and the Higgs field, showing the gauge-parameter independence of the transverse photon propagator and of the Higgs pole mass up to one-loop order. In Sec. IV, we calculate the spectral function of both propagators, and in Sec. V we compare our results with those of a nonunitary

massive Abelian model. We also address the residue computation. Section VI collects our conclusions and outlook.

II. ABELIAN HIGGS MODEL: SOME ESSENTIALS

We start from the Abelian Higgs classical action with a manifest global $U(1)$ symmetry

$$S = \int d^4x \left\{ \frac{1}{4} F_{\mu\nu} F_{\mu\nu} + (D_\mu \varphi)^\dagger D_\mu \varphi + \frac{\lambda}{2} \left(\varphi^\dagger \varphi - \frac{v^2}{2} \right)^2 \right\}, \quad (6)$$

where

$$\begin{aligned} F_{\mu\nu} &= \partial_\mu A_\nu - \partial_\nu A_\mu, \\ D_\mu \varphi &= \partial_\mu \varphi + ie A_\mu \varphi \end{aligned} \quad (7)$$

and the parameter v gives the vacuum expectation value (vev) of the scalar field to first order in \hbar , $\langle \varphi \rangle_0 = v$. The spontaneous symmetry breaking is implemented by expressing the scalar field as an expansion around its vev, namely

$$\varphi = \frac{1}{\sqrt{2}} ((v+h) + i\rho), \quad (8)$$

where the real part h is identified as the Higgs field and ρ is the (unphysical) Goldstone boson, with $\langle \rho \rangle = 0$. Here we choose to expand around the classical value of the vev, so that $\langle h \rangle$ is zero at the classical level but receives loop corrections.¹ The action (6) now becomes

$$\begin{aligned} S = \int d^4x \left\{ \frac{1}{4} F_{\mu\nu} F_{\mu\nu} + \frac{1}{2} \partial_\mu h \partial_\mu h + \frac{1}{2} \partial_\mu \rho \partial_\mu \rho - e\rho \partial_\mu h A_\mu \right. \\ \left. + e(h+v) A_\mu \partial_\mu \rho + \frac{1}{2} e^2 A_\mu [(h+v)^2 + \rho^2] A_\mu \right. \\ \left. + \frac{1}{8} \lambda (h^2 + 2hv + \rho^2)^2 \right\}, \end{aligned} \quad (9)$$

and we notice that both the gauge field and the Higgs field have acquired the following masses:

$$m^2 = e^2 v^2, \quad m_h^2 = \lambda v^2. \quad (10)$$

With this parametrization, the Higgs coupling λ and the parameter v can be fixed in terms of m , m_h and e , whose values will be suitably chosen later in the text.

¹There is of course an equivalent procedure of fixing $\langle h \rangle$ to zero at all orders, by expanding φ around the full vev: $\varphi = \frac{1}{\sqrt{2}} ((\langle \varphi \rangle + h) + i\rho)$. In Appendix B we explicitly show that—as expected—both procedures give the same final results up to a given order.

Even in the broken phase, the action (9) is left invariant by the following gauge transformations:

$$\begin{aligned}\delta A_\mu &= -\partial_\mu \omega, & \delta \varphi &= i\omega \varphi, & \delta \varphi^\dagger &= -i\omega \varphi^\dagger, \\ \delta h &= -e\omega \rho, & \delta \rho &= e\omega(v+h),\end{aligned}\quad (11)$$

where ω is the gauge parameter.

A. Gauge fixing

Quantization of the theory (9) requires a proper gauge fixing. We shall employ the gauge fixing term

$$S_{gf} = \int d^4x \left\{ \frac{1}{2\xi} (\partial_\mu A_\mu + \xi m \rho)^2 \right\}, \quad (12)$$

known as the 't Hooft or R_ξ -gauge, which has the pleasant property of canceling the mixed term $\int d^4x (e v A_\mu \partial_\mu \rho)$ in the expression (9). Of course, (12) breaks the gauge invariance of the action. As is well known, the latter is replaced by the BRST invariance. In fact, introducing the FP ghost fields \bar{c}, c as well as the auxiliary field b , for the BRST transformations, we have

$$\begin{aligned}s A_\mu &= -\partial_\mu c, & s c &= 0, \\ s \varphi &= i e c \varphi, & s \varphi^\dagger &= -i e c \varphi^\dagger, \\ s h &= -e c \rho, & s \rho &= e c (v + h), \\ s \bar{c} &= i b, & s b &= 0.\end{aligned}\quad (13)$$

Importantly, the operator s is nilpotent, i.e., $s^2 = 0$, allowing us to work with the so-called BRST cohomology, a useful concept to prove unitarity and renormalizability of the Abelian Higgs model [48,62,69].

We can now introduce the gauge fixing in a BRST-invariant way via

$$\begin{aligned}S_{gf} &= s \int d^4x \left\{ -i \frac{\xi}{2} \bar{c} b + \bar{c} (\partial_\mu A_\mu + \xi m \rho) \right\}, \quad (14) \\ &= \int d^4x \left\{ \frac{\xi}{2} b^2 + i b \partial_\mu A_\mu + i b \xi m \rho + \bar{c} \partial^2 c \right. \\ &\quad \left. - \xi m^2 \bar{c} c - \xi m e \bar{c} h c \right\}.\end{aligned}\quad (15)$$

Notice that the ghosts (\bar{c}, c) get a gauge parameter-dependent mass while interacting directly with the Higgs field.

The total gauge fixed BRST-invariant action then becomes

$$\begin{aligned}S &= \int d^4x \left\{ \frac{1}{4} F_{\mu\nu} F_{\mu\nu} + \frac{1}{2} \partial_\mu h \partial_\mu h + \frac{1}{2} \partial_\mu \rho \partial_\mu \rho - e \rho \partial_\mu h A_\mu + e h A_\mu \partial_\mu \rho + \frac{1}{2} m^2 A_\mu A_\mu + \frac{1}{2} e^2 A_\mu [h^2 + 2vh + \rho^2] A_\mu \right. \\ &\quad \left. + \frac{1}{8} \lambda (h^2 + \rho^2) (h^2 + \rho^2 + 4hv) + \frac{1}{2} m_h^2 h^2 + m A_\mu \partial_\mu \rho + \frac{\xi}{2} b^2 + i b \partial_\mu A_\mu + i b \xi m \rho + \bar{c} (\partial^2) c - m^2 \xi \bar{c} c - m \xi e \bar{c} h c \right\}, \quad (16)\end{aligned}$$

with

$$sS = 0. \quad (17)$$

In Appendix A we collect the propagators and vertices corresponding to the action (16) of the Abelian Higgs model in the R_ξ gauge.

III. PHOTON AND HIGGS PROPAGATORS AT ONE LOOP

In this section we obtain the one-loop corrections to the photon propagator, as well as to the propagator of the Higgs boson. This requires the calculation,² in Secs. III A and III B, of the Feynman diagrams as shown in Figs. 1 and 2.

Notice that the last four diagrams in Figs. 1 and 2 vanish for $\langle h \rangle = 0$. Since we have chosen to expand the φ field around its classical vev v [cf. (8)], $\langle h \rangle$ has loop

²We have used the techniques of modifying integrals into “master integrals” with momentum-independent numerators from [70].

contributions which are nonzero and the resulting tadpole diagrams have to be included in the quantum corrections for the propagators.³

Of course the final result for the propagators would be the same had we chosen to expand the φ field around its full vev and required $\langle h \rangle = 0$. In fact, including the tadpole diagrams in our formulation has the same effect as shifting the masses of the fields to include the one-loop corrections to the Higgs vev $\langle \varphi \rangle$, calculated by imposing $\langle h \rangle = 0$ (see Appendix B for the technical details). These diagrams can actually be seen as a correction to the tree-level mass term: in the spontaneously broken phase the gauge boson mass is given by $m = e \langle \varphi \rangle$, thus depending on $\langle \varphi \rangle$, which receives quantum corrections order by order. Therefore, the full inverse photon propagator can be written as

³The diagrams with tadpole balloons are not part of the standard definition of one-particle irreducible diagrams that contribute to the self-energies. However, since the momentum flowing in the vertical h -field (dashed) line is zero, they can be effectively included as a momentum-independent term in the self-energies.

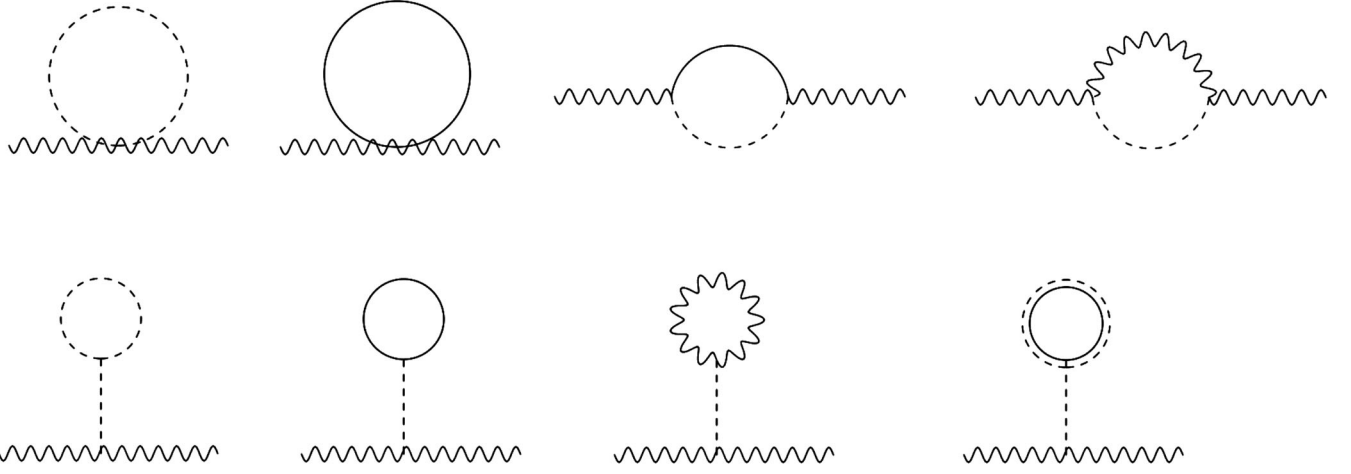


FIG. 1. Contributions to one-loop photon self-energy in the Abelian Higgs model, including tadpole contributions in the second line. Wavy lines represent the photon field, dashed lines the Higgs field, solid lines the Goldstone boson, and double lines the ghost field.

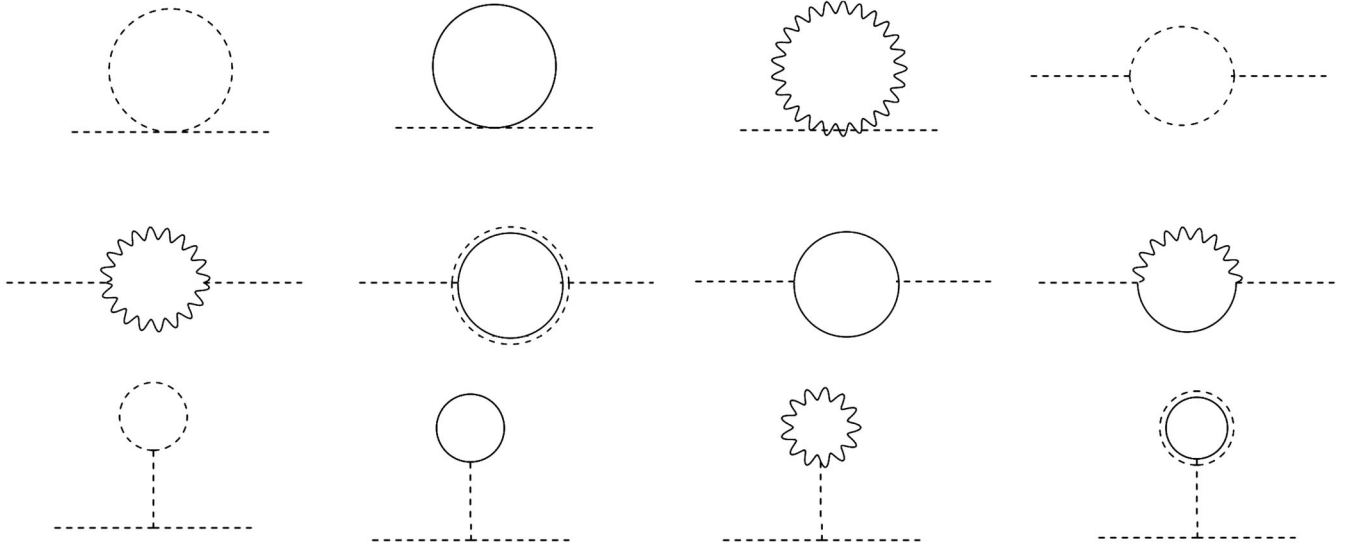


FIG. 2. Contributions to the one-loop Higgs self-energy. Line representations are as in Fig. 1.

$$\begin{aligned}
 G_{AA}^{-1}(p^2) &= p^2 + e^2 v^2 + (\text{1 PI diagrams}) \\
 &+ (\text{diagrams with tadpoles}) \\
 &= p^2 + e^2 \langle \varphi \rangle^2 + (\text{1 PI diagrams}), \quad (18)
 \end{aligned}$$

where the equalities are to be understood up to a given order in perturbation theory and a similar reasoning can be drawn for the Higgs propagator.

In what follows, we proceed with the expansion adopted in (8) and include the tadpole diagrams explicitly in our self-energy results.

The calculations are done for arbitrary dimension d . In Sec. III C we will analyze the results for $d = 4 - \epsilon$, making use of the techniques of dimensional regularization in the $\overline{\text{MS}}$ scheme.

A. Corrections to the photon self-energy

The first diagram contributing to the photon self-energy is the Higgs boson snail (first diagram in the first line of Fig. 1), and it gives a contribution

$$\Gamma_{A_\mu A_\nu,1}(p^2) = \frac{-4e^2}{(4\pi)^{d/2}} \frac{\Gamma(2-d/2)}{2-d} \frac{m_h^{d-2}}{2} \delta_{\mu\nu}. \quad (19)$$

The second diagram is the Goldstone boson snail (second diagram in the first line of Fig. 1)

$$\Gamma_{A_\mu A_\nu,2}(p^2) = \frac{-4e^2}{(4\pi)^{d/2}} \frac{\Gamma(2-d/2)}{2-d} \frac{(\xi m^2)^{d/2-1}}{2} \delta_{\mu\nu}. \quad (20)$$

Being momentum independent, the only effect of these first two diagrams is to renormalize the mass parameters (m_h^2, m^2).

The third term contributing to the photon propagator is the Higgs-Goldstone sunset (third diagram in first line of Fig. 1)

$$\begin{aligned} \Gamma_{A_\mu A_\nu,3}(p^2) &= \frac{4e^2}{(4\pi)^{d/2}} \frac{\Gamma(2-d/2)}{2-d} \int_0^1 dx \left[K_{d/2-1}(m_h^2, \xi m^2) \mathcal{P}_{\mu\nu} \right. \\ &\quad \left. + \left(K_{d/2-1}(m_h^2, \xi m^2) + \frac{(2-d)}{4} (1-4x(1-x)) p^2 K_{d/2-2}(m_h^2, \xi m^2) \right) \mathcal{L}_{\mu\nu} \right], \end{aligned} \quad (21)$$

where we used the definitions

$$K_\alpha(m_1^2, m_2^2) \equiv (p^2 x(1-x) + x m_1^2 + (1-x) m_2^2)^\alpha, \quad (22)$$

and

$$\mathcal{P}_{\mu\nu} = \delta_{\mu\nu} - \frac{P_\mu P_\nu}{p^2}, \quad (23)$$

$$\mathcal{L}_{\mu\nu} = \frac{P_\mu P_\nu}{p^2}, \quad (24)$$

which are the transversal and longitudinal projectors, respectively. The fourth term contributing to the photon propagator is the Higgs-photon sunset (fourth diagram in first line of Fig. 1)

$$\begin{aligned} \Gamma_{A_\mu A_\nu,4}(p^2) &= \frac{4e^2}{(4\pi)^{d/2}} \frac{\Gamma(2-d/2)}{2-d} \int_0^1 dx \left[((2-d)m^2 K_{d/2-2}(m_h^2, m^2) + K_{d/2-1}(m_h^2, m^2) - K_{d/2-1}(m_h^2, \xi m^2)) \mathcal{P}_{\mu\nu} \right. \\ &\quad + ((2-d)m^2 K_{d/2-2}(m_h^2, m^2) + K_{d/2-1}(m_h^2, m^2) - K_{d/2-1}(m_h^2, \xi m^2)) \\ &\quad \left. + (2-d)p^2 x^2 (K_{d/2-2}(m_h^2, m^2) - K_{d/2-1}(m_h^2, \xi m^2)) \mathcal{L}_{\mu\nu} \right]. \end{aligned} \quad (25)$$

Finally, we have four tadpole (balloon) diagrams. The Higgs boson balloon (first diagram of the last line in Fig. 1)

$$\Gamma_{A_\mu A_\nu,5}(p^2) = \frac{4e^2}{(4\pi)^{d/2}} \frac{\Gamma(2-d/2)}{(2-d)} \frac{3}{2} m_h^{d/2-1} \delta_{\mu\nu}, \quad (26)$$

the Goldstone boson balloon (second diagram of the last line in Fig. 1)

$$\Gamma_{A_\mu A_\nu,6}(p^2) = \frac{4e^2}{(4\pi)^{d/2}} \frac{\Gamma(2-d/2)}{(2-d)} \frac{1}{2} (\xi m)^{d/2-1} \delta_{\mu\nu}, \quad (27)$$

the photon balloon (third diagram of the last line in Fig. 1)

$$\begin{aligned} \Gamma_{A_\mu A_\nu,7}(p^2) &= 2e^2 \frac{m^2}{m_h^2} \int \frac{d^d k}{(2\pi)^d} \left(\frac{1}{k^2 + m^2} (d-1) + \frac{\xi}{k^2 + \xi m^2} \right) \delta_{\mu\nu}, \end{aligned} \quad (28)$$

and finally, the ghost balloon (fourth diagram of the last line in Fig. 1)

$$\Gamma_{A_\mu A_\nu,8}(p^2) = -2e^2 \frac{m^2}{m_h^2} \int \frac{d^d k}{(2\pi)^d} \frac{\xi}{k^2 + \xi m^2} \delta_{\mu\nu}. \quad (29)$$

Combining all these contributions (19)–(29), we find

$$\begin{aligned} \Gamma_{A_\mu A_\nu}(p^2) &= \frac{4e^2}{(4\pi)^{d/2}} \frac{\Gamma(2-d/2)}{2-d} \int_0^1 dx \left((2-d)m^2 K_{d/2-2}(m^2, m_h^2) + K_{d/2-1}(m^2, m_h^2) + m_h^{d-2} + \frac{m^d}{m_h^2} (d-1) \right) \mathcal{P}_{\mu\nu} \\ &\quad + \frac{4e^2}{(4\pi)^{d/2}} \frac{\Gamma(2-d/2)}{2-d} \int_0^1 dx \left(\frac{2-d}{4} (1-4x) p^2 K_{d/2-2}(m_h^2, \xi m^2) + (2-d)(m^2 + p^2 x^2) K_{d/2-2}(m_h^2, m^2) \right. \\ &\quad \left. + K_{d/2-1}(m_h^2, m^2) + m_h^{d-2} + \frac{m^d}{m_h^2} (d-1) \right) \mathcal{L}_{\mu\nu}. \end{aligned} \quad (30)$$

Defining

$$\Gamma_{A_\mu A_\nu} = \Pi_{AA}^\perp(p^2) \mathcal{P}_{\mu\nu} + \Pi_{AA}^\parallel(p^2) \mathcal{L}_{\mu\nu}, \quad (31)$$

it follows that

$$\partial_\xi \Pi_{AA}^\perp = 0. \quad (32)$$

As expected, Eq. (32) expresses the gauge parameter independence of the gauge-invariant transverse component of the photon propagator [63]. Then, the connected transverse form factor,

$$G_{AA}^\perp(p^2) = \frac{1}{p^2 + m^2} + \frac{1}{(p^2 + m^2)^2} \Pi_{AA}^\perp(p^2) + \mathcal{O}(e^4), \quad (33)$$

can be rewritten in terms of the resummed form factor as

$$G_{AA}^\perp(p^2) = \frac{1}{p^2 + m^2 - \Pi_{AA}^\perp(p^2) + \mathcal{O}(e^4)}. \quad (34)$$

B. Corrections to the Higgs self-energy

The first diagrams contributing to the Higgs self-energy are of the snail type, renormalizing the masses of the internal fields.

The Higgs boson snail (first diagram in the first line of Fig. 2)

$$\Gamma_{hh,1}(p^2) = -3 \frac{\lambda}{(4\pi)^{d/2}} \frac{\Gamma(2-d/2)}{(2-d)} m_h^{d-2}, \quad (35)$$

the Goldstone boson snail (second diagram in the first line of Fig. 2)

$$\Gamma_{hh,2}(p^2) = -\frac{\lambda}{(4\pi)^{d/2}} \frac{\Gamma(2-d/2)}{(2-d)} (\xi m^2)^{d/2-1} \quad (36)$$

and the photon snail (third diagram in the first line of Fig. 2)

$$\begin{aligned} \Gamma_{hh,3}(p^2) \\ = -2 \frac{e^2}{(4\pi)^{d/2}} \frac{\Gamma(2-d/2)}{(2-d)} ((d-1)m^{d-2} + \xi(\xi m^2)^{d/2-1}). \end{aligned} \quad (37)$$

Next, we observe a couple of sunset diagrams: the Higgs boson sunset (fourth diagram in the first line of Fig. 2)

$$\begin{aligned} \Gamma_{hh,4}(p^2) &= \frac{9}{2} \frac{\lambda}{(4\pi)^{d/2}} \frac{\Gamma(2-d/2)}{(2-d)} (2-d)m_h^2 \\ &\times \int_0^1 dx K_{d/2-2}(m_h^2, m_h^2), \end{aligned} \quad (38)$$

the photon sunset (first diagram in the second line of Fig. 2)

$$\begin{aligned} \Gamma_{hh,5}(p^2) &= e^2 \frac{\Gamma(2-d/2)}{2-d} \frac{1}{(4\pi)^{d/2}} \int_0^1 dx \left[(2-d) \left(2m^2(d-1) + 2p^2 + \frac{p^4}{2m^2} \right) K_{d/2-2}(m^2, m^2) \right. \\ &\quad - (2-d) \left(2p^2 + \frac{p^4}{m^2} + \xi^2 m^2 + 2p^2 \xi - 2\xi m^2 + m^2 \right) K_{d/2-2}(m^2, \xi m^2) \\ &\quad \left. + (2-d) \left(2\xi p^2 + 2\xi^2 m^2 + \frac{p^4}{2m^2} \right) K_{d/2-2}(\xi m^2, \xi m^2) + 2(\xi-1)(m^2)^{d/2-1} + 2(1-\xi)(\xi m^2)^{d/2-1} \right], \end{aligned} \quad (39)$$

the ghost sunset (second diagram in the second line of Fig. 2)

$$\Gamma_{hh,6}(p^2) = -\frac{e^2}{(4\pi)^{d/2}} \frac{\Gamma(2-d/2)}{(2-d)} (2-d)m^2 \xi^2 \int_0^1 dx K_{d/2-2}(\xi m^2, \xi m^2), \quad (40)$$

the Goldstone boson sunset (third diagram in the second line of Fig. 2)

$$\Gamma_{hh,7}(p^2) = \frac{1}{2} \frac{\lambda}{(4\pi)^{d/2}} \frac{\Gamma(2-d/2)}{(2-d)} (2-d)m_h^2 \int_0^1 dx K_{d/2-2}(\xi m^2, \xi m^2)^{d/2-2} \quad (41)$$

and a mixed Goldstone-photon sunset (fourth diagram in the second line of Fig. 2)

$$\begin{aligned} \Gamma_{hh,8}(p^2) &= e^2 \frac{\Gamma(2-d/2)}{2-d} \frac{1}{(4\pi)^{d/2}} \int_0^1 dx \left[(2-d) \left(2p^2 + \frac{p^4}{m^2} + \xi^2 m^2 + 2p^2 \xi - 2\xi m^2 + m^2 \right) K_{d/2-2}(m^2, \xi m^2) \right. \\ &\quad \left. - (2-d) \left(\xi^2 m^2 + \frac{p^4}{m^2} + 2p^2 \xi \right) K_{d/2-2}(\xi m^2, \xi m^2) + 2 \left(1 - \xi - \frac{p^2}{m^2} \right) (m^2)^{d/2-1} + 2 \left(2\xi - 1 + \frac{p^2}{m^2} \right) (\xi m^2)^{d/2-1} \right]. \end{aligned} \quad (42)$$

Finally, we have the tadpole diagrams: the Higgs balloon (first diagram on the third line of Fig. 2)

$$\Gamma_{hh,9}(p^2) = 9 \frac{\lambda}{(4\pi)^{d/2}} \frac{\Gamma(2-d/2)}{(2-d)} m_h^{d-2}, \quad (43)$$

the photon balloon (second diagram on the third line of Fig. 2)

$$\Gamma_{hh,10}(p^2) = 6 \frac{e^2}{(4\pi)^{d/2}} \frac{\Gamma(2-d/2)}{(2-d)} ((d-1)m^{d-2} + \xi(\xi m^2)^{d/2-1}), \quad (44)$$

the Goldstone boson balloon (third diagram on the third line of Fig. 2)

$$\Gamma_{hh,11}(p^2) = 3 \frac{\lambda}{(4\pi)^{d/2}} \frac{\Gamma(2-d/2)}{(2-d)} (\xi m^2)^{d/2-1} \quad (45)$$

and the ghost balloon (fourth diagram on the third line of Fig. 2)

$$\Gamma_{hh,12}(p^2) = -6 \frac{e^2 \xi}{(4\pi)^{d/2}} \frac{\Gamma(2-d/2)}{(2-d)} (\xi m^2)^{d/2-1}. \quad (46)$$

Putting together Eqs. (35) to (46) we find the total one-loop correction to the Higgs boson self-energy,

$$\begin{aligned} \Pi_{hh}(p^2) \equiv \Gamma_{hh}(p^2) &= \frac{\Gamma(2-d/2)}{2-d} \frac{1}{(4\pi)^{d/2}} \int_0^1 dx \left[(2-d)e^2 \left(2m^2(d-1) + 2p^2 + \frac{p^4}{2m^2} \right) K_{d/2-2}(m^2, m^2) \right. \\ &+ \frac{9}{2} \lambda (2-d) m_h^2 K_{d/2-2}(m_h^2, m_h^2) + e^2 \left(-2 \frac{p^2}{m^2} + 4(d-1) \right) (m^2)^{d/2-1} + 6\lambda (m_h^2)^{d/2-1} \\ &\left. + (2-d) \left(-\frac{p^4}{2m^2} e^2 + \frac{\lambda}{2} m_h^2 \right) K_{d/2-2}(\xi m^2, \xi m^2) + 2 \left(\frac{p^2}{m^2} e^2 + \lambda \right) (\xi m^2)^{d/2-1} \right]. \quad (47) \end{aligned}$$

So, for the Higgs boson resummed connected propagator, we find

$$G_{hh}(p^2) = \frac{1}{p^2 + m_h^2 - \Pi_{hh}(p^2)}. \quad (48)$$

C. Results for $d=4-\epsilon$

For $d=4$, the 2-point functions are divergent. We therefore follow the standard procedure of dimensional regularization, as we have no chiral fermions present. Thus, we choose $d=4-\epsilon$ with ϵ an infinitesimal parameter and analyze the solution in the limit $\epsilon \rightarrow 0$.

Let us start with the photon 2-point function, given for arbitrary dimension d by (30). The mass dimension of the coupling constant e is $[e] = 2-d/2 = \epsilon/2$, and redefining $e \rightarrow e\tilde{\mu}^{\epsilon/2} = e\tilde{\mu}^{2-d/2}$ we put the dimension on $\tilde{\mu}$, while e is dimensionless. Using

$$\frac{4e^2}{(4\pi)^{d/2}} \frac{\Gamma(2-d/2)}{2-d} \stackrel{d \rightarrow 4-\epsilon}{=} -2 \frac{e^2}{(4\pi)^2} \left(\frac{2}{\epsilon} + 1 + \ln(\mu^2) \right), \quad (49)$$

where we defined

$$\mu^2 = \frac{4\pi\tilde{\mu}^2}{e^{\gamma_E}}, \quad (50)$$

we find for the divergent part of the transverse photon 2-point function

$$\Pi_{AA,\text{div}}^\perp(p^2) = \frac{2}{\epsilon} \frac{e^2}{(4\pi)^2} \left(\frac{p^2}{3} + 6 \left(\frac{g^2}{\lambda} - \frac{1}{2} \right) m^2 + 3m_h^2 \right), \quad (51)$$

and these infinities are, following the $\overline{\text{MS}}$ scheme, canceled by the corresponding counterterms.

The renormalized correlation function is then finite in the limit $d \rightarrow 4$, and we find for the inverse propagator

$$\begin{aligned} \frac{1}{G_{AA}^\perp(p^2)} &= p^2 + m^2 \\ &- 2 \frac{e^2}{(4\pi)^2} \int_0^1 dx \left\{ K(m^2, m_h^2) \left(1 - \ln \frac{K(m^2, m_h^2)}{\mu^2} \right) \right. \\ &+ m_h^2 \left(1 - \ln \frac{m_h^2}{\mu^2} \right) + \frac{m^4}{m_h^2} \left(1 - 3 \ln \frac{m^2}{\mu^2} \right) \\ &\left. + 2m^2 \ln \frac{K(m^2, m_h^2)}{\mu^2} \right\}, \quad (52) \end{aligned}$$

where we set $K(m_1^2, m_2^2) \equiv K_1(m_1^2, m_2^2)$.

In the same way, we find the divergent part of the Higgs boson 2-point function:

$$\Pi_{hh,\text{div}}(p^2) = -\frac{1}{2\epsilon} \frac{1}{(4\pi)^2} (e^2(12p^2 - 4\xi p^2) + \lambda(8m_h^2 - 4\xi m^2)), \quad (53)$$

which is canceled by the corresponding counterterm. Therefore, the inverse Higgs boson propagator reads

$$\begin{aligned} \frac{1}{G_{hh}(p^2)} = & p^2 + m_h^2 + \frac{1}{(4\pi)^2} \int_0^1 dx \left\{ e^2 \left[p^2 \left(1 - \ln \frac{m^2}{\mu^2} - 2 \ln \frac{K(m^2, m^2)}{\mu^2} \right) \right. \right. \\ & - \left. \frac{p^4}{2m^2} \ln \frac{K(m^2, m^2)}{\mu^2} - 6m^2 \left(1 - \ln \frac{m^2}{\mu^2} + \ln \frac{K(m^2, m^2)}{\mu^2} \right) \right] \\ & + \lambda \left[\frac{1}{2} m_h^2 \left(-6 + 6 \ln \frac{m_h^2}{\mu^2} - 9 \ln \frac{K(m_h^2, m_h^2)}{\mu^2} \right) \right] \\ & \left. - \left[\xi(e^2 p^2 + \lambda m^2) \left(1 - \ln \frac{\xi m^2}{\mu^2} \right) - \left(e^2 \frac{p^4}{2m^2} - \lambda \frac{m_h^2}{2} \right) \ln \frac{K(\xi m^2, \xi m^2)}{\mu^2} \right] \right\}. \quad (54) \end{aligned}$$

Notice that the dependence on the Feynman parameter x in the integrals (52) and (54) is restricted to functions of the type $\int_0^1 dx \ln \frac{K(m_1^2, m_2^2)}{\mu^2}$. These functions have an analytical solution, depicted in Appendix C.

IV. SPECTRAL PROPERTIES OF THE PROPAGATORS

In this section we will investigate the spectral properties corresponding to the connected propagators of the last section. Strictly speaking, the calculation of the spectral properties should only be done to first order⁴ in \hbar , since the one-loop corrections to the propagators have been evaluated up to this order. In practice, however, for small values of the coupling constants the higher-order contributions become negligible, and one could treat the one-loop solution as the all-order solution without a significant numerical difference. Even so, when looking for analytical rather than numerical results—for example a gauge parameter dependence—we should restrict ourselves to the first-order results. We shall see the crucial difference between both approaches.

To plot the spectral properties of our model we choose some specific values of the parameters $\{m, m_h, \mu, e\}$. We want to restrict ourselves to the case where the Higgs particle is a stable particle, so we need $m_h^2 < 4m^2$. Furthermore, given the Abelian nature of the model, and thus a weak coupling regime in the infrared, we can choose an energy scale μ that is sufficiently small w.r.t. the elusive Landau pole (that is exponentially large) and a corresponding small value for the coupling constant e . For the rest of this section and the next, we will therefore choose the

⁴This would correspond to first order in the gauge coupling e^2 and in the Higgs coupling λ neglecting the implicit coupling dependence in the masses.

parameter values $m = 2$ GeV, $m_h = \frac{1}{2}$ GeV, $\mu = 10$ GeV, $e = \frac{1}{10}$. Notice that by choosing μ and e , we are implicitly fixing the Landau pole Λ , with $\mu \ll \Lambda$; see [52] for more details. We have checked that results are as good as independent from the choice of μ over a very wide range of μ -values.

We start by calculating the pole mass in Sec. IV A. The pole mass is the actual physical mass of a particle that enters the energy-momentum dispersion relation. It is an observable for both the photon and the Higgs boson and should therefore not depend on the gauge parameter ξ . We will also discuss the residue to first order and compare these with the output from the Nielsen identities [63]. In Sec. IV B we show how to obtain the spectral function to first order from the propagator. In Sec. IV C we will discuss some more details about the Higgs spectral function.

A. Pole mass, residue and Nielsen identities

The pole mass for any massless or massive field excitation is obtained by calculating the pole of the resummed connected propagator

$$G(p^2) = \frac{1}{p^2 + m^2 - \Pi(p^2)}, \quad (55)$$

where $\Pi(p^2)$ is the self-energy correction. The pole of the propagator is thus equivalently defined by the equation

$$p^2 + m^2 - \Pi(p^2) = 0, \quad (56)$$

and its solution defines the pole mass $p^2 = -m_{\text{pole}}^2$. As consistency requires us to work up to a fixed order in perturbation theory, we should solve Eq. (56) for the pole mass in an iterative fashion. To first order in \hbar , we find

$$m_{\text{pole}}^2 = m^2 - \Pi^{1\text{-loop}}(-m^2) + \mathcal{O}(\hbar^2), \quad (57)$$

where $\Pi^{1\text{-loop}}$ is the first order, or one-loop, correction to the propagator.

Next, we also want to compute the residue Z , again up to order \hbar . In principle, the residue is given by

$$Z = \lim_{p^2 \rightarrow -m_{\text{pole}}^2} (p^2 + m_{\text{pole}}^2) G(p^2). \quad (58)$$

We write (55) in a slightly different way

$$\begin{aligned} G(p^2) &= \frac{1}{p^2 + m^2 - \Pi(p^2)} \\ &= \frac{1}{p^2 + m^2 - \Pi^{1\text{-loop}}(-m^2) - (\Pi(p^2) - \Pi^{1\text{-loop}}(-m^2))} \\ &= \frac{1}{p^2 + m_{\text{pole}}^2 - \tilde{\Pi}(p^2)}, \end{aligned} \quad (59)$$

where we defined $\tilde{\Pi}(p^2) = \Pi(p^2) - \Pi^{1\text{-loop}}(-m^2)$. At one loop, expanding $\tilde{\Pi}(p^2)$ around $p^2 = -m_{\text{pole}}^2 = -m^2 + \mathcal{O}(\hbar)$ gives the residue

$$\begin{aligned} Z &= \frac{1}{1 - \partial_{p^2} \Pi(p^2)|_{p^2 = -m^2}} \\ &= 1 + \partial_{p^2} \Pi(p^2)|_{p^2 = -m^2} + \mathcal{O}(\hbar^2). \end{aligned} \quad (60)$$

In [63], for the Abelian Higgs model, the Nielsen identities were obtained for both the photon and the Higgs boson. It was found that for the photon propagator, the transverse part is explicitly independent of ξ to all orders of perturbation theory, giving the Nielsen identity

$$\partial_\xi (G_{AA}^\perp)^{-1}(p^2) = 0 \quad (61)$$

and consequently

$$\begin{aligned} \partial_\xi \partial_{p^2} (G_{AA}^\perp)^{-1}(p^2)|_{p^2 = -m_{\text{pole}}^2} &= 0, \\ \partial_\xi (G_{AA}^\perp)^{-1}(-m_{\text{pole}}^2) &= 0, \end{aligned} \quad (62)$$

confirming the gauge independence of the residue and the pole mass. Of course, this is not unexpected since the transverse part of an Abelian gauge field propagator can be written as

$$\mathcal{P}_{\mu\nu} \langle A_\mu A_\nu \rangle_{\text{conn}} \propto \langle A_\mu^T A_\mu^T \rangle, \quad A_\mu^T = \mathcal{P}_{\mu\nu} A_\nu \quad (63)$$

and the transverse component A_μ^T is gauge invariant under Abelian gauge transformations.

We can now compare the outcome of the Nielsen identities with our one-loop calculation (52). Indeed, to the first order, Eq. (52) is an explicit demonstration of the identity (61).

For the Higgs boson, the Nielsen identity is a bit more complicated and is given by

$$\partial_\xi G_{hh}^{-1}(p^2) = -\partial_\chi G_{Y_1 h}^{-1}(p^2) G_{hh}^{-1}(p^2), \quad (64)$$

where $G_{Y_1 h}^{-1}(p^2)$ stands for a nonvanishing 1PI Green function which can be obtained from the extended BRST symmetry which also acts on the gauge parameter [65]. To be more precise, Y_1 is a local source coupled to the BRST variation of the Higgs field [see (13)], while χ is coupled to the integrated composite operator $\int d^4x (-\frac{i}{2} \bar{c} b + m c \rho)$. Acting with ∂_χ inserts the latter composite operator with zero momentum flow into the 1PI Green function $\langle (sh)h \rangle$; see [63] for the explicit expression of $G_{Y_1 h}^{-1}(p^2)$ in terms of Feynman diagrams.

As a consequence, the Higgs propagator $G_{hh}(p^2)$ is not gauge independent, in agreement with our results (54). From (64) we further find

$$\begin{aligned} \partial_\xi \partial_{p^2} G_{hh}^{-1}(p^2)|_{p^2 = -m_{\text{pole}}^2} \\ = -\partial_\chi G_{Y_1 h}^{-1}(-m_{\text{pole}}^2) \partial_{p^2} G_{hh}^{-1}(p^2)|_{p^2 = -m_{\text{pole}}^2}, \end{aligned} \quad (65)$$

which means that the residue is not gauge independent, as $G_{Y_1 h}^{-1}(p^2)$ does not necessarily vanish at the pole. We can confirm this for the one-loop calculation; see Fig. 3.

Furthermore, we have

$$\partial_\xi G_{hh}^{-1}(-m_{\text{pole}}^2) = 0, \quad (66)$$

so that the Higgs pole mass is indeed gauge independent, the expected result for the physical (observable) Higgs mass. This can be confirmed to one-loop order by using Eq. (57); see also Fig. 6. Explicitly, in Eq. (54) for $G_{hh}^{-1}(-m_h^2)$ all the gauge parameter dependence drops out, which means that the Higgs pole mass is gauge independent to first order in \hbar .

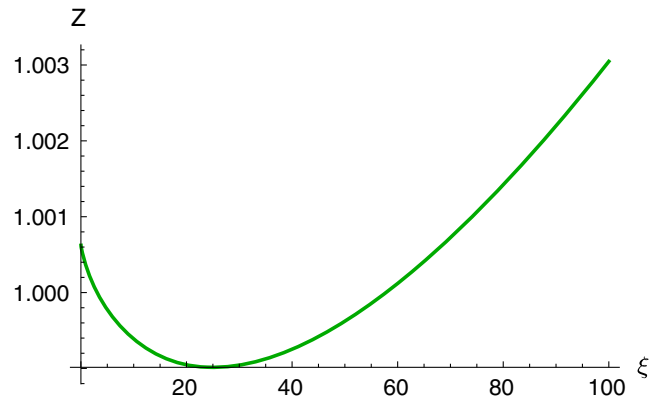


FIG. 3. Gauge dependence of the residue of the pole for the Higgs field, for the parameter values $m = 2$ GeV, $m_h = \frac{1}{2}$ GeV, $\mu = 10$ GeV, $e = \frac{1}{10}$.

B. Obtaining the spectral function

We can try to determine the spectral functions themselves to first order. To do so, we compare the Källén-Lehmann spectral representation for the propagator

$$G(p^2) = \int_0^\infty dt \frac{\rho(t)}{t + p^2}, \quad (67)$$

where $\rho(t)$ is the spectral density function, with the propagator (59) to first order, written as

$$\begin{aligned} G(p^2) &= \frac{Z}{(p^2 + m_{\text{pole}}^2 - \tilde{\Pi}(p^2))Z} \\ &= \frac{Z}{p^2 + m_{\text{pole}}^2 - \tilde{\Pi}(p^2) + (p^2 + m_{\text{pole}}^2) \left. \frac{\partial \tilde{\Pi}(p^2)}{\partial p^2} \right|_{p^2 = -m^2}} \\ &= \frac{Z}{p^2 + m_{\text{pole}}^2} \\ &\quad + Z \left(\frac{\tilde{\Pi}(p^2) - (p^2 + m_{\text{pole}}^2) \left. \frac{\partial \tilde{\Pi}(p^2)}{\partial p^2} \right|_{p^2 = -m^2}}{(p^2 + m_{\text{pole}}^2)^2} \right), \quad (68) \end{aligned}$$

where in the last line we used a first-order Taylor expansion so that the propagator has an isolated pole at $p^2 = -m_{\text{pole}}^2$. In (67) we can isolate this pole in the same way, by defining the spectral density function as $\rho(t) = Z\delta(t - m_{\text{pole}}^2) + \tilde{\rho}(t)$, giving

$$G(p^2) = \frac{Z}{p^2 + m_{\text{pole}}^2} + \int_0^\infty dt \frac{\tilde{\rho}(t)}{t + p^2}, \quad (69)$$

and we identify the second term in each of the representations (68) and (69) as the reduced propagator

$$\tilde{G}(p^2) \equiv G(p^2) - \frac{Z}{p^2 + m_{\text{pole}}^2}, \quad (70)$$

so that

$$\begin{aligned} \tilde{G}(p^2) &= \int_0^\infty dt \frac{\tilde{\rho}(t)}{t + p^2} \\ &= Z \left(\frac{\tilde{\Pi}(p^2) - (p^2 + m_{\text{pole}}^2) \left. \frac{\partial \tilde{\Pi}(p^2)}{\partial p^2} \right|_{p^2 = -m^2}}{(p^2 + m_{\text{pole}}^2)^2} \right). \quad (71) \end{aligned}$$

Finally, using Cauchy's integral theorem in complex analysis, we can find $\tilde{\rho}(t)$ as a function of $\tilde{G}(p^2)$, giving

$$\tilde{\rho}(t) = \frac{1}{2\pi i} \lim_{\epsilon \rightarrow 0^+} (\tilde{G}(-t - i\epsilon) - \tilde{G}(-t + i\epsilon)). \quad (72)$$

We can now extract the spectral functions for the photon and the Higgs boson. Therefore, we first calculate the pole masses up to first order, using Eq. (56). For our parameter values, we find the photon pole mass up to first order in \hbar to

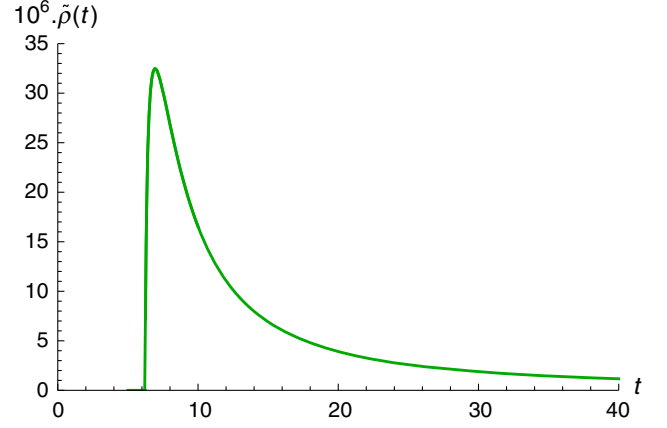


FIG. 4. The reduced spectral function of the photon, with t given in GeV^2 , for the parameter values $m = 2 \text{ GeV}$, $m_h = \frac{1}{2} \text{ GeV}$, $\mu = 10 \text{ GeV}$, $e = \frac{1}{10}$. The first-order pole mass lies at $t = 4.08286 \text{ GeV}^2$, and the two-particle state of one photon field and one Higgs field starts at $t^* = (m_h + m)^2 = 6.25 \text{ GeV}^2$.

be $m_{AA,\text{pole}}^2 = 4.08286 \text{ GeV}^2$. In Fig. 4 one finds the spectral function for the photon propagator, which is, as expected, positive definite, in addition to being ξ independent. The threshold (branch point) of the propagator is given by $t^* = (m_h + m)^2$, which can be read off from (52): it corresponds to the smallest value of $-p^2$ where $K(m^2, m_h^2)$ becomes negative.

For the Higgs field, we find the pole mass up to first order in \hbar to be $m_{hh,\text{pole}}^2 = 0.251665 \text{ GeV}^2$. The Higgs spectral function, however, is gauge dependent, and therefore it cannot have any direct physical interpretation. As an illustration, we plot the Higgs spectral function for different values of the gauge parameter in Fig. 5. For small values of t , the spectral functions for different gauge parameter values are as good as identical, with a two-particle state for two Higgs particles starting at $t^* = (m_h + m_h)^2 = 1 \text{ GeV}^2$ and a photon two-particle state starting at $t^* = (m + m)^2 = 16 \text{ GeV}^2$. For larger t , significant differences appear for different values of ξ since the threshold for the two-particle state for the Goldstone boson is given by $t^* = (\sqrt{\xi}m + \sqrt{\xi}m)^2$. Of course, this two-particle state is highly unphysical because the Goldstone field does not represent a physical particle, something which is reflected in the fact that it gives a descending contribution to the spectral function. For $\xi < 3$, we even find that this descending behavior causes the spectral function to become negative. We will relate this to the asymptotic behavior of the Higgs propagator in the next section, along with some other salient features of the Higgs spectral properties, including its threshold.

C. Some subtleties of the Higgs spectral function

In this section we discuss some subtleties that arose during the analysis of the spectral function of the Higgs boson.

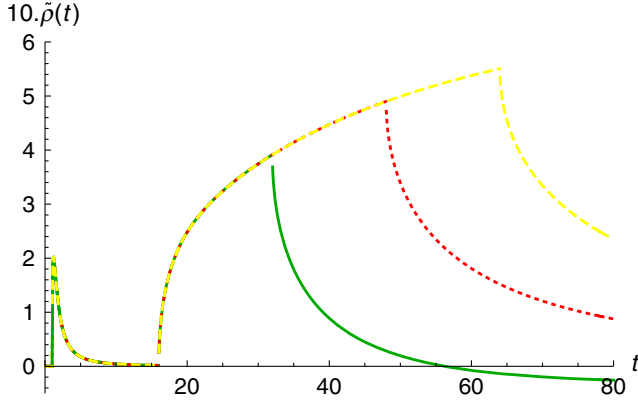


FIG. 5. The reduced spectral function of the Higgs boson, with t given in GeV^2 , for $\xi = 2$ (green, solid), $\xi = 3$ (red, dotted), $\xi = 4$ (yellow, dashed) and the parameter values $m = 2 \text{ GeV}$, $m_h = \frac{1}{2} \text{ GeV}$, $\mu = 10 \text{ GeV}$, $e = \frac{1}{10}$. The first-order pole mass lies at $t = 0.251665 \text{ GeV}^2$. The threshold for the Higgs two-particle state is given at $t^* = (m_h + m_h)^2 = 1 \text{ GeV}^2$ and for the photon two-particle state at $t^* = (m + m)^2 = 16 \text{ GeV}^2$. We find a (negative) Goldstone two-particle state at $t^* = (\sqrt{\xi}m + \sqrt{\xi}m)^2$, corresponding to $t^* = (32 \text{ GeV}^2, 48 \text{ GeV}^2, 64 \text{ GeV}^2)$ for $\xi = (2, 3, 4)$.

1. A slightly less correct approximation for the pole mass

In the previous two sections we have obtained strictly first-order expressions. In practice, for small values of the coupling parameter e^2 , we could think about making the approximation

$$G(p^2) = \frac{1}{p^2 + m^2 - \Pi(p^2)} \approx \frac{1}{p^2 + m^2 - \Pi^{1\text{-loop}}(p^2)}, \quad (73)$$

in which case one can fix the pole mass by locating the root of

$$p^2 + m^2 - \Pi^{1\text{-loop}}(p^2) = 0. \quad (74)$$

The difference between the pole masses obtained by the iterative method (57) and the approximation (74) is very small, of the order 10^{-6} GeV for our set of parameters. However, it is rather interesting to notice that the pole mass of the Higgs boson becomes gauge dependent in the approximation (74). This is no surprise, as the validity of the Nielsen identities is understood either in an exact way or in a consistent order-by-order approximation. The above discussed approximation is neither.

In Fig. 6 one can see the gauge dependence of the approximated pole mass of the Higgs, in contrast with the first order pole mass. Even worse, for very small values of ξ , the approximated pole mass gets complex (conjugate) values. This is due to the fact that the threshold of the branch cut, the branch point, for (47) is ξ dependent, as we will see in the next section.

2. Something more on the branch points

The existence of a diagram with two internal Goldstone lines (see Fig. 2) leads to a term proportional to $\int_0^1 dx \ln(p^2 x(1-x) + \xi m^2)$ in the Higgs propagator (47). This means that for small values of ξ , the threshold for the branch cut of the propagator will be ξ dependent too. Let us look at the Landau gauge $\xi = 0$. In this gauge, the above \ln term is proportional to $\ln(p^2)$, due to the now massless Goldstone bosons. This logarithm has a branch point at $p^2 = 0$, meaning that the pole mass will be lying on the branch cut. Since the first-order pole mass is real and gauge independent, this means that $\Pi_{hh}^{1\text{-loop}}(-m_h^2)$ is a singular real point on the branch cut. In the slightly less correct approximation of the last section, we will find complex conjugate poles as in Fig. 6. This is explained by the fact that for every real value different from $p^2 = -m_h^2$, we are on the branch cut; see Fig. 7.

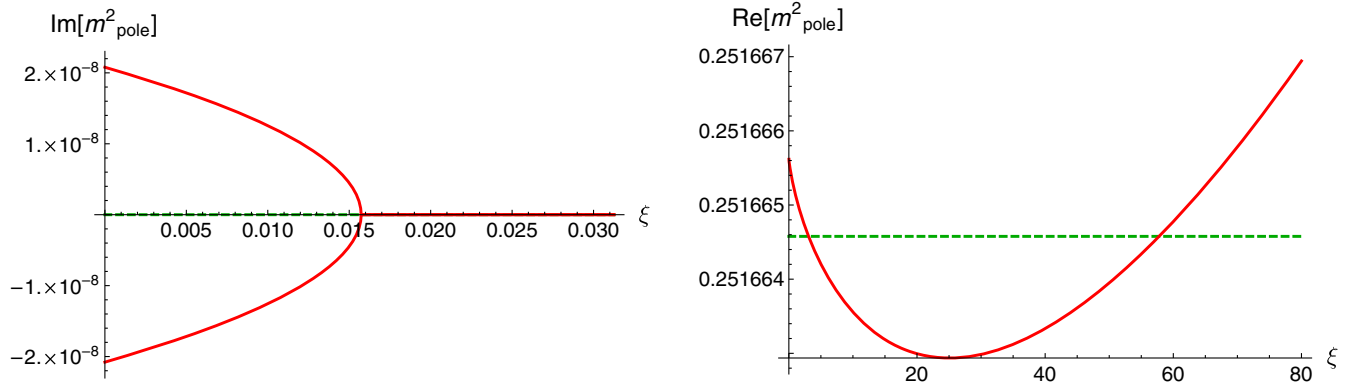


FIG. 6. Gauge dependence of the Higgs pole mass obtained iteratively to first order (green) and the approximated pole mass (red), for the parameter values $m = 2 \text{ GeV}$, $m_h = \frac{1}{2} \text{ GeV}$, $\mu = 10 \text{ GeV}$, $e = \frac{1}{10}$. The right panel shows the real part; the left panel shows the imaginary part.

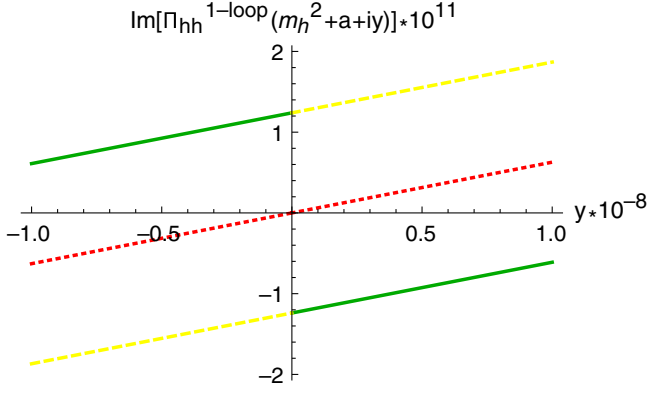


FIG. 7. Behavior of the one-loop correction of the Higgs propagator $\Pi_{hh}(p^2)$ around the pole mass, for the values $a = -10^{-6}$ (yellow, dashed), $a = 0$ (red, dotted), $a = 10^{-6}$ (green, solid). The value x is a small imaginary variation of the argument in $\Pi_{hh}(p^2)$. Only for $a = 0$ do we find a continuous function at $x = 0$, meaning that for any other value, we are on the branch cut.

Another consequence of the fact that, for small ξ , the pole mass is a real point inside the branch cut is that $\Pi_{hh}(p^2)$ is nondifferentiable at $p^2 = -m_h^2$, and we cannot extract a residue for this pole. In order to avoid such a problem, we should move away from the Landau gauge and take a larger value for ξ , so that the threshold for the branch cut will be smaller than $-m_h^2$. For this we need $4\xi m^2 > m_h^2$, which, in the case of our parameters set, means requiring that $\xi > \frac{1}{64}$, in accordance with Fig. 6.

3. Asymptotics of the spectral function

Away from the Landau gauge, we see on Fig. 5 that for e.g., $\xi = 2$ the Higgs spectral function is not nonpositive everywhere, while for e.g., $\xi = 4$ it is positive definite, with a turning point at $\xi = 3$. How can we explain this difference? The answer can be related to the UV behavior of the propagator. For $p^2 \rightarrow \infty$, the Higgs boson propagator at one loop behaves as

$$G_{hh}(p^2) = \frac{\mathcal{Z}}{p^2 \ln \frac{p^2}{\mu^2}}, \quad (75)$$

with \mathcal{Z} depending on the gauge parameter ξ . Now, one can show (see Appendix D) that for $\mathcal{Z} > 0$, $\rho(t)$ becomes negative for a large value of t . For our parameter set, we find that for large momenta

$$G_{hh}^{-1}(p^2) \rightarrow (3 - \xi) \frac{p^2 \ln(p^2)}{1600\pi^2}, \quad \text{for } p^2 \rightarrow \infty, \quad (76)$$

so that for $\xi < 3$, we indeed find $\mathcal{Z} > 0$. This indicates that the large momentum behavior of the propagator makes a difference around $\xi = 3$ and determines the positivity of the

spectral function, a known fact [53,71,72]. This being said, at the same time we cannot trust the propagator values for $p^2 \rightarrow \infty$ without taking into account the renormalization group (RG) effects and, in particular, the running of the coupling, which is problematic for nonasymptotically free gauge theories such as the Abelian Higgs model.

V. A NONUNITARY $U(1)$ MODEL

In this section, we discuss an Abelian model of the Curci-Ferrari (CF) type [73], in order to compare it with the Higgs model (1). Both models are massive $U(1)$ models with a BRST symmetry. However, while the BRST operator s of the Higgs model is nilpotent, this is not true for the CF-like model. We know that the Higgs model is unitary but, by the criterion of [48], the CF model is most probably not.

In Sec. VA we discuss some essentials for the CF-like model: the action with the modified BRST symmetry, tree-level propagators and vertices. In Sec. VB we discuss the one-loop propagators for the photon and scalar field and extract the spectral function. In Sec. VC we introduce a local composite field operator that is left invariant by the modified BRST symmetry of the CF model. The spectral properties of this composite state's propagator will tell us something about the (non)unitarity of the model, since for unitary models, we expect the propagator of a BRST-invariant composite operator to be gauge parameter independent and the spectral function to be positive definite.

A. CF-like $U(1)$ model: Some essentials

We start with the action of the CF-like $U(1)$ model

$$S_{\text{CF}} = \int d^d x \left\{ \frac{1}{4} F_{\mu\nu} F_{\mu\nu} + \frac{m^2}{2} A_\mu A_\mu + (D_\mu \varphi)^\dagger D_\mu \varphi + m_\varphi^2 \varphi^\dagger \varphi + \lambda (\varphi \varphi^\dagger)^2 - \alpha \frac{b^2}{2} + b \partial_\mu A_\mu + \bar{c} \partial^2 c - am^2 \bar{c} c \right\}, \quad (77)$$

where the mass term $\frac{m^2}{2} A_\mu A_\mu$ is put in by hand rather than coming from a spontaneous symmetry breaking, and we have fixed the gauge in the linear covariant gauge with gauge parameter α . The mass term breaks the BRST symmetry (13) in a soft way. This Abelian CF action is, however, invariant under the modified BRST symmetry, $s_m S_{\text{CF}} = 0$, with⁵

⁵This is the Abelian version of the variation (5). For computational purposes, we have also made a rescaling $ib \rightarrow b$. Notice that higher order α -dependent terms present in the CF model are absent in the Abelian limit [42,43].

$$\begin{aligned}
s_m A_\mu &= -\partial_\mu c, & s_m c &= 0, & s_m \varphi &= iec\varphi, \\
s_m \varphi^\dagger &= -iec\varphi^\dagger, & s_m \bar{c} &= b, & s_m b &= -m^2 c.
\end{aligned} \quad (78)$$

As noticed in our Introduction, this modified BRST symmetry is not nilpotent since $s_m^2 \bar{c} \neq 0$.

From the quadratic part of (77) we find the following propagators at tree level:

$$\begin{aligned}
\langle A_\mu(p) A_\nu(-p) \rangle &= \frac{1}{p^2 + m^2} P_{\mu\nu} + \frac{\alpha}{p^2 + \alpha m^2} \mathcal{L}_{\mu\nu}, \\
\langle A_\mu(p) b(-p) \rangle &= i \frac{P_\mu}{p^2 + \alpha m^2}, \\
\langle b(p) b(-p) \rangle &= -\frac{m^2}{p^2 + \alpha m^2}, \\
\langle \varphi^\dagger(p) \varphi(-p) \rangle &= \frac{1}{p^2 + m_\varphi^2}, \\
\langle \bar{c}(p) c(-p) \rangle &= -\frac{1}{p^2 + \alpha m^2},
\end{aligned} \quad (79)$$

while from the interaction terms we find the vertices

$$\begin{aligned}
\Gamma_{A_\mu \varphi^\dagger \varphi}(-p_1, -p_2, -p_3) &= e(p_{3,\mu} - p_{2,\mu}) \delta(p_1 + p_2 + p_3), \\
\Gamma_{A_\mu A_\nu \varphi^\dagger \varphi}(-p_1, -p_2, -p_3, -p_4) &= -2e^2 \delta_{\mu\nu} \delta(p_1 + p_2 + p_3 + p_4), \\
\Gamma_{\varphi^\dagger \varphi \varphi^\dagger \varphi}(-p_1, -p_2, -p_3, -p_4) &= -4\lambda \delta(p_1 + p_2 + p_3 + p_4).
\end{aligned} \quad (80)$$

B. Propagators and spectral functions

The one-loop corrections to the photon and scalar self-energies are given in Figs. 8 and 9. Without going through the calculational details, we directly give here the

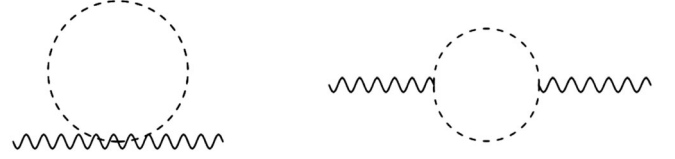


FIG. 8. Contributions to one-loop CF photon self-energy. Wavy lines represent the photon field, and dashed lines represent the scalar field.

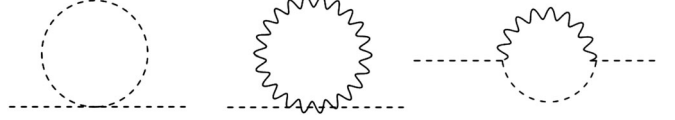


FIG. 9. Contributions to the one-loop CF scalar self-energy. Line representation as in Fig. 8.

propagators in $d = 4$ and discuss some curiosities. The inverse connected photon propagator,

$$\begin{aligned}
(G_{AA}^1)^{-1}(p^2) &= p^2 + m^2 + \frac{e^2}{(4\pi)^2} \int_0^1 dx K(m_\varphi^2, m_\varphi^2) \\
&\times \left(1 - \ln \frac{K(m_\varphi^2, m_\varphi^2)}{\mu^2} \right) - m_\varphi^2 \left(1 - \ln \frac{m_\varphi^2}{\mu^2} \right),
\end{aligned} \quad (81)$$

is independent of the gauge parameter. The threshold of the branch cut is given by $t^* = -4m_\varphi^2$, and to avoid a pole mass lying on the branch cut, we need to choose $m^2 < 4m_\varphi^2$. Choosing $m = \frac{1}{2}$ GeV, $m_\varphi = 2$ GeV, $\mu = 10$ GeV, $e = \frac{1}{10}$, we find a positive spectral function; see Fig. 10.

More interestingly, the scalar propagator

$$\begin{aligned}
G_{\varphi\varphi}^{-1}(p) &= p^2 + m_\varphi^2 - \frac{e^2}{(4\pi)^2} \int_0^1 dx \left(m^2 - \alpha^2 m^2 - \alpha K(m_\varphi^2, m^2) \left(1 - 2 \ln \frac{K(m_\varphi^2, \alpha m^2)}{\mu^2} \right) + 4K(m_\varphi^2, 0) \frac{p^2}{m^2} \left(1 - \ln \frac{K(m_\varphi^2, 0)}{\mu^2} \right) \right. \\
&- 2K(m_\varphi^2, m^2) \frac{p^2}{m^2} \left(1 - \ln \frac{K(m_\varphi^2, m^2)}{\mu^2} \right) - 2K(m_\varphi^2, \alpha m^2) \frac{p^2}{m^2} \left(1 - \ln \frac{K(m_\varphi^2, \alpha m^2)}{\mu^2} \right) + 8 \frac{p^4}{m^2} x^2 \ln \frac{K(m_\varphi^2, 0)}{\mu^2} \\
&- 4 \frac{p^4}{m^2} x^2 \ln \frac{K(m_\varphi^2, m^2)}{\mu^2} - 4p^2 \ln \frac{K(m_\varphi^2, m^2)}{\mu^2} - \left(4\alpha p^2 x - \alpha p^2 x^2 + 4 \frac{p^4}{m^2} x^2 \right) \ln \frac{K(m_\varphi^2, \alpha m^2)}{\mu^2} - 3m^2 \ln \frac{m^2}{\mu^2} \\
&\left. + \alpha m^2 \ln \frac{\alpha m^2}{\mu^2} \right) + \frac{\lambda}{(4\pi)^2} m_\varphi^2 \left(1 - \ln \frac{m_\varphi^2}{\mu^2} \right)
\end{aligned} \quad (82)$$

is α dependent, and so is the iterative first-order pole mass $m_{\varphi, \text{pole}}^2 = m_\varphi^2 - \Pi^{1\text{-loop}}(-m_\varphi^2)$. This field thus cannot represent a physical particle. For any value other than the Landau gauge $\alpha = 0$, we furthermore get complex poles; see Fig. 11.

From the fact that we find gauge-dependent (complex) pole masses for the scalar field, we can already draw the conclusion that the CF model does not describe a physical scalar field. In the next section we will explicitly verify the nonunitarity of this model in yet another way.

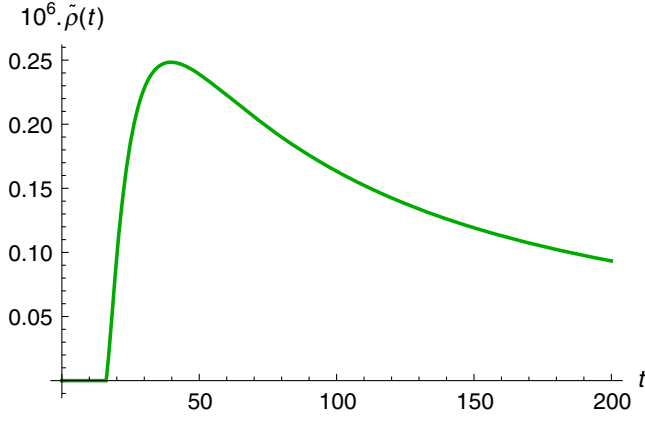


FIG. 10. The reduced spectral function of the photon field in the Abelian CF model, with t given in GeV^2 , for the parameter values $m = 2 \text{ GeV}$, $m_h = \frac{1}{2} \text{ GeV}$, $\mu = 10 \text{ GeV}$, $e = \frac{1}{10}$. The first-order pole mass lies at $t = 0.25151 \text{ GeV}^2$. The photon two-particle state starts at $t^* = (m_\phi + m_\phi)^2 = 16 \text{ GeV}^2$.

Essentially, our findings so far mean that in the CF setting, the unphysical gauge parameter α plays quite an important role here, just like the coupling: different values of the gauge parameter label different theories. This can also be seen from another example: the one-loop vacuum energy of the model will now not only depend on m but also on α .

C. Gauge-invariant operator

The Abelian CF model allows us to construct a BRST-invariant composite operator $(\frac{b^2}{2} + m^2 \bar{c}c)$, with

$$s_m \left(\frac{b^2}{2} + m^2 \bar{c}c \right) = 0. \quad (83)$$

Although $s_m^2 \neq 0$ and we can therefore no longer introduce the BRST cohomology classes, we can still use the fact that s_m is a symmetry generator, thereby defining a would-be physical subspace as the one being annihilated by s_m .

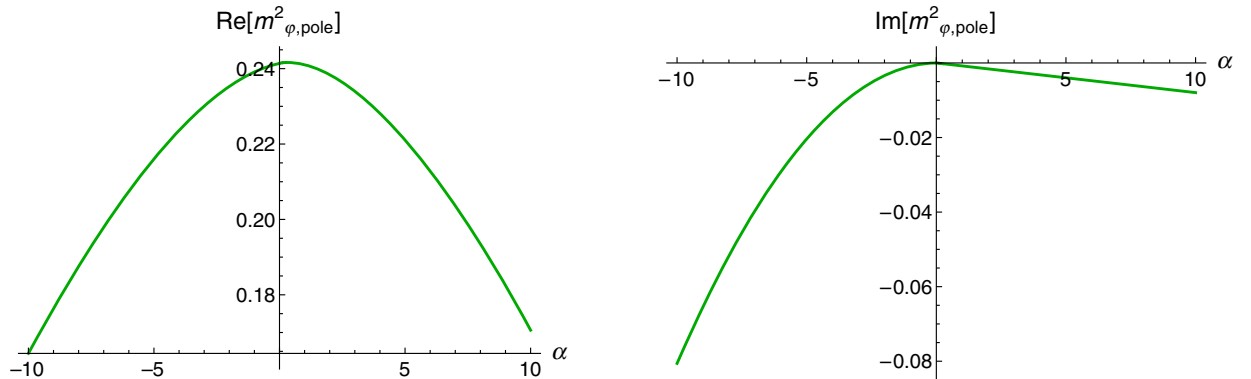


FIG. 11. Gauge dependence of the first order pole mass for the scalar field. The left panel shows the real part; the right panel shows the imaginary part. The chosen parameter values are $m = 2 \text{ GeV}$, $m_\phi = \frac{1}{2} \text{ GeV}$, $\mu = 10 \text{ GeV}$, $e = \frac{1}{10}$.

A Fock space analogue of this operator was introduced in [49], where it was established that it has a negative norm. As a consequence, it was shown that the physical subspace relating to the symmetry generator s_m was not well defined, as it contains ghost states. Several more such states were identified later in [50].

Up to leading order, the connected propagator of the composite operator in Eq. (83) reads

$$\begin{aligned} G_{\frac{b^2}{2} + m^2 \bar{c}c}(p^2) &= \left\langle \left(\frac{b^2}{2} + m^2 \bar{c}c \right), \left(\frac{b^2}{2} + m^2 \bar{c}c \right) \right\rangle \\ &= \frac{1}{4} \langle b^2, b^2 \rangle + m^4 \langle \bar{c}c, \bar{c}c \rangle. \end{aligned} \quad (84)$$

We thus find the propagator (84) to be

$$\begin{aligned} G_{\frac{b^2}{2} + m^2 \bar{c}c}(p^2) &= -\frac{3}{4} m^2 \int \frac{d^d k}{(2\pi)^d} \frac{1}{k^2 + \alpha m^2} \frac{1}{(k-p)^2 + \alpha m^2} \\ &= -\frac{3}{4} m^2 \frac{1}{(4\pi)^{d/2}} \Gamma(2 - d/2) \\ &\quad \times \int_0^1 dx K_{d/2-2}(\alpha m^2, \alpha m^2), \end{aligned} \quad (85)$$

and this gives, for $d = 4$, using the $\overline{\text{MS}}$ -scheme,

$$G_{\frac{b^2}{2} + m^2 \bar{c}c}(p^2) = \frac{3}{4} \frac{m^2}{(4\pi)^2} \int_0^1 dx \ln \left(\frac{K(\alpha m^2, \alpha m^2)}{\mu^2} \right). \quad (86)$$

Clearly, the propagator depends on the gauge parameter α , a not so welcome feature for a presumably physical object.

We can also find the spectral function immediately from the propagator by again relying on (72). In Fig. 12, one sees that the spectral function is negative for different values of α . Both the α dependence and the negative definiteness of the spectral functions demonstrate the nonunitarity of the Abelian CF model. To our knowledge, this is the first time that ghost-dependent invariant operators in the physical subspace of a CF model have been constructed from the

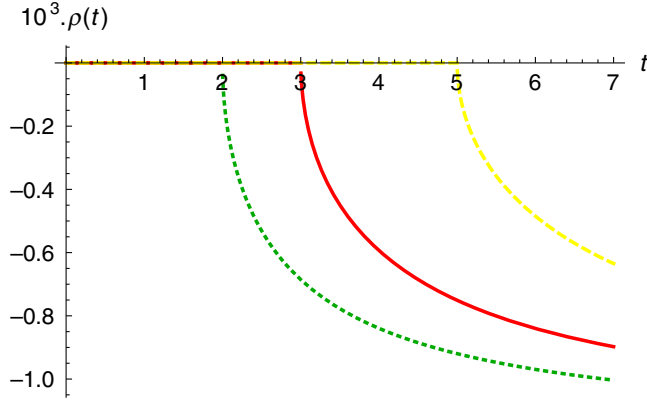


FIG. 12. The spectral function of the composite operator $\frac{b^2}{2} + m^2 \bar{c}c$, for $\alpha = 2$ (green, dotted), $\alpha = 3$ (red, solid), $\alpha = 5$ (yellow, dashed). The chosen parameter values are $m = \frac{1}{2}$ GeV, $\mu = 10$ GeV. The threshold for the branch cut of the propagator is given by $t^* = (\sqrt{am} + \sqrt{am})^2$, with $t^* = (2 \text{ GeV}^2, 3 \text{ GeV}^2, 5 \text{ GeV}^2)$ for $\xi = (2, 3, 5)$.

functional viewpoint,⁶ complementing the (asymptotic) Fock space analyses of [49,50].

VI. CONCLUSION AND OUTLOOK

In the present work we have studied the Källén-Lehmann spectral properties of the $U(1)$ Abelian Higgs model in the R_ξ gauge and those of a $U(1)$ CF-like model.

Our main aim was to disentangle, in this analytical, gauge-fixed setup, what is physical and what is not at the level of the elementary particle propagators, in conjunction with the Nielsen identities. Special attention was given to the role played by gauge (in)dependence of different quantities and by the correct implementation of the results up to a given order in perturbation theory. In particular, calculating the spectral function for the Higgs propagator in the $U(1)$ model, it became apparent that an unphysical occurrence of complex poles, as well as a gauge-dependent pole mass, is caused by the use of the resummed (approximate) propagator being exact. Indeed, for small coupling constants, the one-loop correction gives a good approximation of the all-order loop correction, and this is a much used method to find numerical results [19,37,54]. However, for analytical purposes, one should stick to the order at which one has calculated the propagator. As we have illustrated, at least in the $U(1)$ Abelian Higgs model case, one will then find a real and gauge-independent pole mass for the Higgs boson, in accordance with what the Nielsen identities dictate [63].

⁶A similar result can be checked to hold for the original non-Abelian CF model, by adding a few higher order terms to the Abelian operator introduced here. This means that a non-Abelian version of the operator (83), invariant under the BRST transformation (5), can be written down.

Another issue we faced was the fact that the branch point for the Higgs propagator is ξ dependent, being located at $p^2 = 0$ for the Landau gauge $\xi = 0$. For small values of ξ , the pole mass has a real value. However, its value is located on the branch cut, making it impossible to define a residue at this point, and therefore a spectral function. This means that in order to formulate a spectral function, we should move away from the Landau gauge. These issues with unphysical (gauge-variant) thresholds are nothing new; see for example [74]. They reinforce in a natural way the need to work with gauge-invariant field operators to correctly describe the observable excitations of a gauge theory.

For the photon, the (transverse) propagator is gauge independent (even BRST invariant), and consequently so are the pole mass, residue, and spectral function. For the Higgs boson, the propagator, residue, and spectral function are gauge dependent, while the pole mass is gauge independent, in line with the latter being an observable quantity. Notice that the residue of the two-point function does not need to be gauge independent since this does not follow from the Nielsen identities, as we discussed in our main text. Rather, the Nielsen identities can be used to show that the residues of the pole masses in S -matrix elements are gauge independent, that is, the residues of the singularities in observable scattering amplitudes; see [75,76]. These residues can evidently be different per scattering process (and per different mass pole). The fact that the Higgs propagator is gauge dependent is not surprising, given that the Higgs field is not invariant under the Abelian gauge transformation.

In future work, it would be interesting to consider, even in perturbation theory, gauge-invariant operators and study their spectral properties using the same techniques of this paper. If the elementary fields are not gauge invariant (like the Higgs field, but also the gluon field in QCD), these aforementioned gauge-invariant operators will turn out to be composite in nature. Such an approach has recently been addressed in [77,78], based on the seminal observations of Fröhlich-Morchio-Strocchi [79,80], in which composite operators with the same global quantum numbers (parity, spin, ...) as the elementary particles are constructed.⁷ These composite states will enable us to access directly the physical spectrum of the theory. Moreover, we notice that the spectral properties and the behavior in the complex momentum plane of a (gauge-invariant) composite operator will nontrivially depend on the spectral properties of its gauge-variant constituents. This gives another motivation why it is meaningful to study spectral properties of gauge-variant

⁷For a recent discussion of the renormalization properties of higher dimensional gauge-invariant operators in Yang-Mills Higgs models, see the recent results by [59].

propagators. Another nice illustrative example of this interplay is the Bethe-Salpeter study of glueballs in pure gauge theories [81], based on spectral properties of constituent gluons and ghosts [3]. We further notice that working with gauge-invariant variables will also evade the above-mentioned problem with unphysical (gauge-variant) thresholds. Moreover, this methodology could also shed more light on how the confinement-like and Higgs-like phases are analytically connected in the (coupling, Higgs vev) diagram in the case of a non-Abelian Higgs field in the fundamental representation, thereby making contact with the lattice predictions of Fradkin-Shenker [82,83].

In conclusion, in this work several tools have been worked out to determine spectral properties in perturbation theory. We worked up to first order in \hbar , but everything can be consistently extended to higher orders. We paid attention to how to avoid problems with complex poles and to the important pivotal role of the Nielsen identities, which are intimately related to the exact nilpotent BRST invariance of the model. These tools will turn out to be quite useful for forthcoming work on the spectral properties of Higgs-Yang-Mills theories. For these theories, the Nielsen identities are well established [66], with supporting lattice data [84], thus providing a solid foundation with which to compare any results.

ACKNOWLEDGMENTS

The authors would like to thank the Brazilian agencies Conselho Nacional de Desenvolvimento Científico e Tecnológico (CNPq) and Fundação de Amparo à Pesquisa do Estado do Rio de Janeiro (FAPERJ) for financial support. This study was financed in part by the Coordenação de Aperfeiçoamento de Pessoal de Nível Superior—Brasil (CAPES)—Financial Code 001 (M. N. F.). This paper is also part of the project Instituto Nacional de Ciência e Tecnologia – Física Nuclear e Aplicações (INCT-FNA) Process No. 464898/2014-5.

APPENDIX A: PROPAGATORS AND VERTICES OF THE ABELIAN HIGGS MODEL IN THE R_ξ GAUGE

1. Field propagators

The quadratic part of the action (16) in the bosonic sector is given by

$$S_{\text{bos}}^{\text{quad}} = \frac{1}{2} \int d^4x \{ A_\mu (-\delta_{\mu\nu}(\partial^2 - m^2) + \partial_\mu \partial_\nu) A_\nu - \rho \partial^2 \rho - h(\partial^2 - m_h^2)h + \bar{c}(\partial^2 - m^2)\xi c + 2ib\partial_\mu A_\mu + \xi b^2 + 2im\xi b\rho + 2mA_\mu \partial_\mu \rho \}. \quad (\text{A1})$$

Putting this in a matrix form yields

$$S_{\text{bos}}^{\text{quad}} = \frac{1}{2} \int d^4x \Psi_\mu^T \mathcal{O}_{\mu\nu} \Psi_\nu, \quad (\text{A2})$$

where

$$\Psi_\mu^T = (A_\mu \quad b \quad \rho \quad h), \quad \Psi_\nu = \begin{pmatrix} A_\nu \\ b \\ \rho \\ h \end{pmatrix}, \quad (\text{A3})$$

and

$$\mathcal{O} = \begin{pmatrix} (-\delta_{\mu\nu}(\partial^2 - m^2) + \partial_\mu \partial_\nu) & -i\partial_\mu & m\partial_\mu & 0 \\ i\partial_\nu & \xi & im\xi & 0 \\ -m\partial_\nu & im\xi & -\partial^2 & 0 \\ 0 & 0 & 0 & -(\partial^2 - m_h^2) \end{pmatrix}. \quad (\text{A4})$$

The tree-level field propagators can be read off from the inverse of \mathcal{O} , leading to the following expressions:

$$\begin{aligned} \langle A_\mu(p) A_\nu(-p) \rangle &= \frac{1}{p^2 + m^2} \mathcal{P}_{\mu\nu} + \frac{\xi}{p^2 + \xi m^2} \mathcal{L}_{\mu\nu}, \\ \langle \rho(p) \rho(-p) \rangle &= \frac{1}{p^2 + \xi m^2}, \\ \langle h(p) h(-p) \rangle &= \frac{1}{p^2 + m_h^2}, \\ \langle A_\mu(p) b(-p) \rangle &= \frac{p_\mu}{p^2 + \xi m^2}, \\ \langle b(p) \rho(-k) \rangle &= \frac{-im}{p^2 + \xi m^2}, \end{aligned} \quad (\text{A5})$$

where $\mathcal{P}_{\mu\nu} = \delta_{\mu\nu} - \frac{p_\mu p_\nu}{p^2}$ and $\mathcal{L}_{\mu\nu} = \frac{p_\mu p_\nu}{p^2}$ are the transversal and longitudinal projectors, respectively. The ghost propagator is

$$\langle \bar{c}(p) c(-p) \rangle = \frac{1}{p^2 + \xi m^2}. \quad (\text{A6})$$

2. Vertices

From the action (16), we find the following vertices:

$$\begin{aligned}
\Gamma_{A_\mu \rho h}(-p_1, -p_2, -p_3) &= ie(p_{\mu,3} - p_{\mu,2})\delta(p_1 + p_2 + p_3), \\
\Gamma_{A_\mu A_\nu h}(-p_1, -p_2, -p_3) &= -2e^2 v \delta_{\mu\nu} \delta(p_1 + p_2 + p_3), \\
\Gamma_{A_\mu A_\nu hh}(-p_1, -p_2, -p_3, -p_4) &= -2e^2 \delta_{\mu\nu} \delta(p_1 + p_2 + p_3 + p_4), \\
\Gamma_{A_\mu A_\nu \rho \rho}(-p_1, -p_2, -p_3, -p_4) &= -2e^2 \delta_{\mu\nu} \delta(p_1 + p_2 + p_3 + p_4), \\
\Gamma_{hhhh}(-p_1, -p_2, -p_3, -p_4) &= -3\lambda \delta(p_1 + p_2 + p_3 + p_4), \\
\Gamma_{hh\rho\rho}(-p_1, -p_2, -p_3, -p_4) &= -\lambda \delta(p_1 + p_2 + p_3 + p_4), \\
\Gamma_{\rho\rho\rho\rho}(-p_1, -p_2, -p_3, -p_4) &= -3\lambda \delta(p_1 + p_2 + p_3 + p_4), \\
\Gamma_{hhh}(-p_1, -p_2, -p_3) &= -3\lambda v \delta(p_1 + p_2 + p_3), \\
\Gamma_{h\rho\rho}(-p_1, -p_2, -p_3) &= -\lambda v \delta(p_1 + p_2 + p_3), \\
\Gamma_{\bar{c}hc}(-p_1, -p_2, -p_3) &= -m\xi e \delta(p_1 + p_2 + p_3).
\end{aligned} \tag{A7}$$

APPENDIX B: EQUIVALENCE BETWEEN INCLUDING TADPOLE DIAGRAMS IN THE SELF-ENERGIES AND SHIFTING $\langle \varphi \rangle$

There is yet another way to come to (47). For this, we do not need to include the balloon-type tadpoles in the self-energies but rather fix the expectation value of the Higgs field $\langle h \rangle = 0$ by shifting the vacuum expectation value of the Higgs field to its proper one-loop value. The h field one-point function has the following contributions at one-loop order:

(i) the gluon contribution

$$-\frac{1}{m_h^2} \frac{2e^2 v}{(4\pi)^{d/2}} \frac{\Gamma(2-d/2)}{(2-d)} (m^{d-2}(d-1) + \xi(\xi m^2)^{d/2-1}), \tag{B1}$$

(ii) the Goldstone boson one

$$-\frac{1}{m_h^2} \lambda v \frac{1}{(4\pi)^{d/2}} \frac{\Gamma(2-d/2)}{(2-d)} (\xi m^2)^{d/2-1}, \tag{B2}$$

(iii) the ghost loop

$$2 \frac{1}{m_h^2} \frac{e^2 v \xi}{(4\pi)^{d/2}} \frac{\Gamma(2-d/2)}{(2-d)} (\xi m^2)^{d/2-1}, \tag{B3}$$

(iv) the Higgs boson one

$$-3 \frac{1}{m_h^2} \frac{\lambda v}{(4\pi)^{d/2}} \frac{\Gamma(2-d/2)}{(2-d)} m_h^{d-2}. \tag{B4}$$

Together those four contributions yield

$$\Gamma_{\langle h \rangle} = \frac{1}{(4\pi)^{d/2}} \frac{\Gamma(2-d/2)}{(2-d)} \frac{1}{m_h^2} (-2e^2 v m^{d-2}(d-1) - \lambda v (\xi m^2)^{d/2-1} - 3\lambda v m_h^{d-2}), \tag{B5}$$

which becomes, for $d = 4 - \epsilon$,

$$\begin{aligned}
&= -\frac{1}{2} \frac{1}{m_h^2} \frac{1}{(4\pi)^2} \left(\frac{2}{\epsilon} + 1 + \ln(\mu^2) \right) \\
&\quad \times (-2e^2 v m^{2-\epsilon}(3-\epsilon) - \lambda v (\xi m^2)^{1-\epsilon/2} - 3\lambda v m_h^{2-\epsilon})
\end{aligned} \tag{B6}$$

$$\begin{aligned}
&= -\frac{1}{2} \frac{1}{m_h^2} \frac{1}{(4\pi)^2} \left(\frac{2}{\epsilon} + 1 + \ln(\mu^2) \right) \\
&\quad \times \left(-2e^2 v m^2 \left(1 - \frac{\epsilon}{2} \ln m^2 \right) (3-\epsilon) - \lambda v \xi m^2 \left(1 - \frac{\epsilon}{2} \ln m^2 \right) \right. \\
&\quad \left. - 3\lambda v m_h^2 \left(1 - \frac{\epsilon}{2} \ln m_h^2 \right) \right).
\end{aligned} \tag{B7}$$

We can split this into a divergent part

$$\Gamma_{\langle h \rangle}^{\text{div}} = \frac{1}{\epsilon} \frac{1}{m_h^2} (6e^2 m^2 v + 3m_h^2 v \lambda + \xi m^2 v), \tag{B8}$$

which we can cancel with the counterterms, and a finite part that reads

$$\Gamma_{\langle h \rangle}^{\text{fin}} = \frac{1}{m_h^2 (4\pi)^2} v \left(m^2 \left(1 - 3 \ln \frac{m^2}{\mu^2} \right) + \frac{1}{m_h^2 (4\pi)^2} \frac{\lambda}{2} v \left(3m_h^2 \left(1 - \ln \frac{h^2}{\mu^2} \right) + \xi m^2 \left(1 - \ln \frac{\xi m^2}{\mu^2} \right) \right) \right). \quad (\text{B9})$$

Now, to see how this reflects on the propagator, we can rewrite our scalar field as

$$\varphi = \frac{1}{\sqrt{2}} ((\langle \varphi \rangle + h) + i\rho), \quad (\text{B10})$$

where the vacuum expectation value of the Higgs field has tree-level and one-loop terms:

$$\langle \varphi \rangle = v + \hbar v_1. \quad (\text{B11})$$

Thus the ‘‘classical’’ potential part of the action becomes

$$\frac{\lambda}{2} \left(\varphi^\dagger \varphi - \frac{v^2}{2} \right)^2 = \frac{\lambda}{8} (\langle \varphi \rangle^2 - v^2 + 2h\langle \varphi \rangle + h^2 + \rho^2)^2, \quad (\text{B12})$$

and expanding this, we find for the shifted tree-level Higgs mass

$$m_h^2 = \frac{1}{2} \lambda (3\langle \varphi \rangle^2 - v^2) = \lambda v^2 + 3\hbar \lambda v v_1, \quad (\text{B13})$$

while the photon mass is

$$m^2 = e^2 \langle \varphi \rangle^2 = e^2 v^2 + 2\hbar e^2 v v_1. \quad (\text{B14})$$

Since now, by construction, $\langle h \rangle = 0$, we can fix the one-loop correction⁸ to the Higgs vev by requiring it to absorb the tadpole contributions:

$$v_1 + \Gamma_{\langle h \rangle}^{\text{fin}} = 0, \quad (\text{B15})$$

and thus

$$v_1 = -\frac{1}{m_h^2 (4\pi)^2} v \left(m^2 \left(1 - 3 \ln \frac{m^2}{\mu^2} \right) - \frac{1}{m_h^2 (4\pi)^2} \frac{\lambda}{2} v \left(3m_h^2 \left(1 - \ln \frac{h^2}{\mu^2} \right) + \xi m^2 \left(1 - \ln \frac{\xi m^2}{\mu^2} \right) \right) \right). \quad (\text{B16})$$

Implementing this in the transverse $\langle AA \rangle$ -propagator, one gets

$$G_{AA}^\perp(p^2) = \frac{1}{p^2 + e^2(v^2 + 2\hbar v_1 v) - \Pi_{AA}^\perp(p^2)}, \quad (\text{B17})$$

where in the correction Π_{AA}^\perp , which is already of $\mathcal{O}(\hbar)$, we only include the $\mathcal{O}(\hbar^0)$ part of $\langle \varphi \rangle$, i.e., v .

We can now verify the ξ -independence of the transverse propagator $\langle AA \rangle$. The ξ -dependent part of $\Pi_{AA}^\perp(p^2)$ is

$$\Pi_{AA,\xi}^\perp(p^2) = \frac{-2e^2}{(4\pi)^{d/2}} \frac{\Gamma(2-d/2)}{2-d} (\xi m^2)^{d/2-1}, \quad (\text{B18})$$

while we find the ξ -dependent part of v_1 to be [using (B5)]

$$v_{1\xi} = \frac{1}{(4\pi)^{d/2}} \frac{\Gamma(2-d/2)}{(2-d)} \frac{1}{m_h^2} (\lambda v (\xi m^2)^{d/2-1}). \quad (\text{B19})$$

In the denominator of (B17) we now easily see that

$$2e^2 v_{1\xi} v_0 - \Pi_{AA,\xi}^\perp(p^2) = 0, \quad (\text{B20})$$

thereby establishing the gauge independence of the transverse photon propagator.

For the Higgs propagator, we similarly find

$$G_{hh}(p^2) = \frac{1}{p^2 + \lambda(v^2 + 3\hbar v_1 v) - \Pi_{hh}(p^2)}. \quad (\text{B21})$$

Here we observe that the ξ -dependent part of v_1 has the same effect as the balloon tadpole of the Goldstone boson (45), consequently establishing the gauge parameter independence of the Higgs mass pole.

APPENDIX C: FEYNMAN INTEGRALS

The integrals over the Feynman parameter x that appear in the field propagators can be done in an exact way, since for general masses m_1, m_2 , we find

$$\int_0^1 dx \ln \frac{K(m_1^2, m_2^2)}{\mu^2} = \frac{1}{2p^2} \left\{ m_1^2 \ln \left(\frac{m_2^2}{m_1^2} \right) + m_2^2 \ln \left(\frac{m_1^2}{m_2^2} \right) + p^2 \ln \left(\frac{m_1^2 m_2^2}{\mu^4} \right) - 2\sqrt{-m_1^4 + 2m_1^2 m_2^2 - 2m_1^2 p^2 - m_2^4 - 2m_2^2 p^2 - p^4} \tan^{-1} \left[\frac{-m_1^2 + m_2^2 - p^2}{\sqrt{-m_1^4 + 2m_1^2(m_2^2 - p^2) - (m_2^2 + p^2)^2}} \right] + 2\sqrt{-m_1^4 + 2m_1^2 m_2^2 - 2m_1^2 p^2 - m_2^4 - 2m_2^2 p^2 - p^4} \tan^{-1} \left[\frac{-m_1^2 + m_2^2 + p^2}{\sqrt{-m_1^4 + 2m_1^2(m_2^2 - p^2) - (m_2^2 + p^2)^2}} \right] - 4p^2 \right\}. \quad (\text{C1})$$

⁸This procedure is also equivalent to computing $\langle \varphi \rangle$ via an effective potential minimization up to the same order.

with $K(m_1, m_2)$ given by

$$K(m_1^2, m_2^2) \equiv (p^2 x(1-x) + x m_1^2 + (1-x)m_2^2). \quad (\text{C2})$$

APPENDIX D: ASYMPTOTICS OF THE HIGGS PROPAGATOR

At one loop, the Higgs propagator behaves like

$$G_{hh}(p^2) = \frac{\mathcal{Z}}{p^2 \ln \frac{p^2}{\mu^2}} \quad \text{for } p^2 \rightarrow \infty. \quad (\text{D1})$$

For $\mathcal{Z} > 0$, this can only be compatible with

$$G_{hh}(p^2) = \int_0^\infty \frac{\rho(t) dt}{t + p^2} \quad (\text{D2})$$

if the superconvergence relation [6,71] $\int dt \rho(t) = 0$ holds, which forbids a positive spectral function. Let us support this nonpositivity of $\rho(t)$ by using (D1) to show that $\rho(t)$ is certainly negative for very large t . This argument can also be found in the Appendix of [5].

Since for a KL representation we have

$$\rho(t) = \frac{1}{2\pi i} \lim_{\epsilon \rightarrow 0^+} (G(-t - i\epsilon) - G(-t + i\epsilon)), \quad (\text{D3})$$

we find for $t \rightarrow +\infty$ and $\epsilon \rightarrow 0^+$,

$$\begin{aligned} \rho(t) &= \frac{\mathcal{Z}}{2\pi i} \left[\frac{(\ln \frac{-t-i\epsilon}{\mu^2})^{-1}}{-t-i\epsilon} - \frac{(\ln \frac{-t+i\epsilon}{\mu^2})^{-1}}{-t+i\epsilon} \right] \\ &= \frac{\mathcal{Z}}{2\pi i t} \left[-\left(\ln \frac{t}{\mu^2} - i\pi \right)^{-1} + \left(\ln \frac{t}{\mu^2} + i\pi \right)^{-1} \right] \\ &= \frac{\mathcal{Z}}{\pi t} \text{Im} \left[\left(\ln \frac{t}{\mu^2} + i\pi \right)^{-1} \right] \\ &= \frac{\mathcal{Z}}{\pi t} \left(\left(\ln \frac{t}{\mu^2} \right)^2 + \pi^2 \right)^{-1/2} \sin \left(-\arctan \frac{\pi}{\ln \frac{t}{\mu^2}} \right). \quad (\text{D4}) \end{aligned}$$

From the latter expression, we can indeed infer that $\rho(t)$ becomes negative for large t . We find

$$\rho(t) \stackrel{t \rightarrow \infty}{\approx} -\frac{\mathcal{Z}}{t} \left(\ln \frac{t}{\mu^2} \right)^{-2} < 0 \quad (\text{D5})$$

for $\mathcal{Z} > 0$, and vice versa for $\mathcal{Z} < 0$.

-
- [1] P.O. Bowman, U.M. Heller, D.B. Leinweber, M.B. Parappilly, A. Sternbeck, L. von Smekal, A.G. Williams, and J.-b. Zhang, Scaling behavior and positivity violation of the gluon propagator in full QCD, *Phys. Rev. D* **76**, 094505 (2007).
- [2] A. Cucchieri, T. Mendes, and A.R. Taurines, Positivity violation for the lattice Landau gluon propagator, *Phys. Rev. D* **71**, 051902 (2005).
- [3] S. Strauss, C.S. Fischer, and C. Kellermann, Analytic Structure of the Landau Gauge Gluon Propagator, *Phys. Rev. Lett.* **109**, 252001 (2012).
- [4] D. Dudal, O. Oliveira, and P.J. Silva, Källén-Lehmann spectroscopy for (un)physical degrees of freedom, *Phys. Rev. D* **89**, 014010 (2014).
- [5] D. Dudal, O. Oliveira, M. Roelfs, and P. Silva, Spectral representation of lattice gluon and ghost propagators at zero temperature, [arXiv:1901.05348](https://arxiv.org/abs/1901.05348).
- [6] J.M. Cornwall, Positivity violations in QCD, *Mod. Phys. Lett. A* **28**, 1330035 (2013).
- [7] G. Krein, C.D. Roberts, and A.G. Williams, On the implications of confinement, *Int. J. Mod. Phys. A* **07**, 5607 (1992).
- [8] C.D. Roberts and A.G. Williams, Dyson-Schwinger equations and their application to hadronic physics, *Prog. Part. Nucl. Phys.* **33**, 477 (1994).
- [9] P. Lowdon, Non-perturbative constraints on the quark and ghost propagators, *Nucl. Phys.* **B935**, 242 (2018).
- [10] I. Montvay and G. Munster, *Quantum Fields on a Lattice*, Cambridge Monographs on Mathematical Physics (Cambridge University Press, Cambridge, England, 1997).
- [11] V.N. Gribov, Quantization of nonabelian gauge theories, *Nucl. Phys.* **B139**, 1 (1978).
- [12] N. Vandersickel and D. Zwanziger, The Gribov problem and QCD dynamics, *Phys. Rep.* **520**, 175 (2012).
- [13] D. Zwanziger, Local and renormalizable action from the Gribov horizon, *Nucl. Phys.* **B323**, 513 (1989).
- [14] D. Zwanziger, Renormalizability of the critical limit of lattice gauge theory by BRS invariance, *Nucl. Phys.* **B399**, 477 (1993).
- [15] D. Dudal, J.A. Gracey, S.P. Sorella, N. Vandersickel, and H. Verschelde, A refinement of the Gribov-Zwanziger approach in the Landau gauge: Infrared propagators in harmony with the lattice results, *Phys. Rev. D* **78**, 065047 (2008).
- [16] J. Serreau and M. Tissier, Lifting the Gribov ambiguity in Yang-Mills theories, *Phys. Lett. B* **712**, 97 (2012).
- [17] M.A.L. Capri, D. Fiorentini, M.S. Guimaraes, B.W. Mintz, L.F. Palhares, S.P. Sorella, D. Dudal, I.F. Justo, A.D. Pereira, and R.F. Sobreiro, More on the

- nonperturbative Gribov-Zwanziger quantization of linear covariant gauges, *Phys. Rev. D* **93**, 065019 (2016).
- [18] D. Zwanziger, Nonperturbative Landau gauge and infrared critical exponents in QCD, *Phys. Rev. D* **65**, 094039 (2002).
- [19] M. Tissier and N. Wschebor, An Infrared Safe perturbative approach to Yang-Mills correlators, *Phys. Rev. D* **84**, 045018 (2011).
- [20] A. Cucchieri and T. Mendes, What's up with IR gluon and ghost propagators in Landau gauge? A puzzling answer from huge lattices, *Proc. Sci.*, LATTICE2007 (2007) 297.
- [21] I. L. Bogolubsky, E. M. Ilgenfritz, M. Muller-Preussker, and A. Sternbeck, Lattice gluodynamics computation of Landau gauge Green's functions in the deep infrared, *Phys. Lett. B* **676**, 69 (2009).
- [22] A. Maas, More on Gribov copies and propagators in Landau-gauge Yang-Mills theory, *Phys. Rev. D* **79**, 014505 (2009).
- [23] A. Cucchieri and T. Mendes, Landau-gauge propagators in Yang-Mills theories at $\beta = 0$: Massive solution versus conformal scaling, *Phys. Rev. D* **81**, 016005 (2010).
- [24] V. G. Bornyakov, V. K. Mitrushkin, and M. Muller-Preussker, $SU(2)$ lattice gluon propagator: Continuum limit, finite-volume effects and infrared mass scale m_{IR} , *Phys. Rev. D* **81**, 054503 (2010).
- [25] O. Oliveira and P. J. Silva, The lattice Landau gauge gluon propagator: Lattice spacing and volume dependence, *Phys. Rev. D* **86**, 114513 (2012).
- [26] A. G. Duarte, O. Oliveira, and P. J. Silva, Lattice gluon and ghost propagators, and the strong coupling in pure $SU(3)$ Yang-Mills theory: Finite lattice spacing and volume effects, *Phys. Rev. D* **94**, 014502 (2016).
- [27] D. Dudal, O. Oliveira, and P. J. Silva, High precision statistical Landau gauge lattice gluon propagator computation vs. the GribovZwanziger approach, *Ann. Phys. (Amsterdam)* **397**, 351 (2018).
- [28] P. Boucaud, F. De Soto, K. Raya, J. Rodríguez-Quintero, and S. Zafeiropoulos, Discretization effects on renormalized gauge-field Greens functions, scale setting, and the gluon mass, *Phys. Rev. D* **98**, 114515 (2018).
- [29] J. M. Cornwall, Dynamical mass generation in continuum QCD, *Phys. Rev. D* **26**, 1453 (1982).
- [30] G. Parisi and R. Petronzio, On low-energy tests of QCD, *Phys. Lett.* **94B**, 51 (1980).
- [31] C. W. Bernard, Monte Carlo evaluation of the effective gluon mass, *Phys. Lett.* **108B**, 431 (1982).
- [32] D. Binosi, D. Ibanez, and J. Papavassiliou, The all-order equation of the effective gluon mass, *Phys. Rev. D* **86**, 085033 (2012).
- [33] A. C. Aguilar, D. Binosi, and J. Papavassiliou, Renormalization group analysis of the gluon mass equation, *Phys. Rev. D* **89**, 085032 (2014).
- [34] A. K. Cyrol, L. Fister, M. Mitter, J. M. Pawłowski, and N. Strodthoff, Landau gauge Yang-Mills correlation functions, *Phys. Rev. D* **94**, 054005 (2016).
- [35] M. Q. Huber, Nonperturbative properties of Yang-Mills theories, Habilitation, University of Graz, 2018.
- [36] P. Boucaud, J. P. Leroy, A. L. Yaouanc, J. Micheli, O. Pene, and J. Rodriguez-Quintero, The infrared behaviour of the pure Yang-Mills Green functions, *Few Body Syst.* **53**, 387 (2012).
- [37] M. Tissier and N. Wschebor, Infrared propagators of Yang-Mills theory from perturbation theory, *Phys. Rev. D* **82**, 101701 (2010).
- [38] J. Gracey, M. Peláez, U. Reinosa, and M. Tissier, Two loop calculation of Yang-Mills propagators in the Curci-Ferrari model, [arXiv:1905.07262](https://arxiv.org/abs/1905.07262).
- [39] G. Comitini and F. Siringo, Variational study of mass generation and deconfinement in Yang-Mills theory, *Phys. Rev. D* **97**, 056013 (2018).
- [40] M. Frasca, Quantum Yang-Mills field theory, *Eur. Phys. J. Plus* **132**, 38 (2017); Erratum, *Eur. Phys. J. Plus* **132**, 242(E) (2017).
- [41] F. Siringo, Analytic structure of QCD propagators in Minkowski space, *Phys. Rev. D* **94**, 114036 (2016).
- [42] G. Curci and R. Ferrari, On a class of Lagrangian models for massive and massless Yang-Mills fields, *Nuovo Cimento A* **32**, 151 (1976).
- [43] F. Delduc and S. P. Sorella, A note on some nonlinear covariant gauges in Yang-Mills theory, *Phys. Lett. B* **231**, 408 (1989).
- [44] M. Peláez, M. Tissier, and N. Wschebor, Two-point correlation functions of QCD in the Landau gauge, *Phys. Rev. D* **90**, 065031 (2014).
- [45] U. Reinosa, J. Serreau, M. Tissier, and N. Wschebor, Deconfinement transition in $SU(2)$ Yang-Mills theory: A two-loop study, *Phys. Rev. D* **91**, 045035 (2015).
- [46] U. Reinosa, J. Serreau, M. Tissier, and A. Tresmontant, Yang-Mills correlators across the deconfinement phase transition, *Phys. Rev. D* **95**, 045014 (2017).
- [47] M. Peláez, M. Tissier, and N. Wschebor, Three-point correlation functions in Yang-Mills theory, *Phys. Rev. D* **88**, 125003 (2013).
- [48] T. Kugo and I. Ojima, Local covariant operator formalism of nonabelian gauge theories and quark confinement problem, *Prog. Theor. Phys. Suppl.* **66**, 1 (1979).
- [49] I. Ojima, Comments on massive and massless Yang-Mills Lagrangians with a quartic coupling of Faddeev-Popov ghosts, *Z. Phys. C* **13**, 173 (1982).
- [50] J. de Boer, K. Skenderis, P. van Nieuwenhuizen, and A. Waldron, On the renormalizability and unitarity of the Curci-Ferrari model for massive vector bosons, *Phys. Lett. B* **367**, 175 (1996).
- [51] M. E. Peskin and D. V. Schroeder, *An Introduction to Quantum Field Theory* (Addison-Wesley, Reading, USA, 1995).
- [52] N. Irges and F. Koutroulis, Renormalization of the Abelian-Higgs model in the R_ξ and unitary gauges and the physicality of its scalar potential, *Nucl. Phys.* **B924**, 178 (2017); Erratum, *Nucl. Phys.* **B938**, 957(E) (2019).
- [53] R. Oehme and W. Zimmermann, Quark and gluon propagators in quantum chromodynamics, *Phys. Rev. D* **21**, 471 (1980).
- [54] Y. Hayashi and K.-I. Kondo, Complex poles and spectral function of Yang-Mills theory, *Phys. Rev. D* **99**, 074001 (2019).
- [55] R. J. Eden, P. V. Landshoff, D. I. Olive, and J. C. Polkinghorne, *The Analytic S-Matrix* (Cambridge University Press, Cambridge, England, 1966).

- [56] L. Baulieu, D. Dudal, M. S. Guimaraes, M. Q. Huber, S. P. Sorella, N. Vandersickel, and D. Zwanziger, Gribov horizon and i-particles: About a toy model and the construction of physical operators, *Phys. Rev. D* **82**, 025021 (2010).
- [57] A. Windisch, M. Q. Huber, and R. Alkofer, On the analytic structure of scalar glueball operators at the Born level, *Phys. Rev. D* **87**, 065005 (2013).
- [58] K.-I. Kondo, M. Watanabe, Y. Hayashi, R. Matsudo, and Y. Suda, Reflection positivity and complex analysis of the Yang-Mills theory from a viewpoint of gluon confinement, [arXiv:1902.08894](https://arxiv.org/abs/1902.08894).
- [59] D. Binosi and R.-A. Tripolt, Spectral functions of confined particles, [arXiv:1904.08172](https://arxiv.org/abs/1904.08172).
- [60] F. Gieres, Symmetries in Physics, in *Proceedings of the fifth "Seminaire Rhodanien de Physique", Dolomieu 1997*, edited by F. Gieres, M. Kibler, C. Lucchesi, and O. Piguet, (Editions Frontieres, 1998).
- [61] G. 't Hooft, C. Itzykson, A. Jaffe, H. Lehmann, P. K. Mitter, I. M. Singer, and R. Stora, Recent developments in gauge theories, *NATO Sci. Ser. B* **59**, 1 (1980).
- [62] C. Becchi, A. Rouet, and R. Stora, Renormalization of the Abelian Higgs-Kibble model, *Commun. Math. Phys.* **42**, 127 (1975).
- [63] R. Haussling and E. Kraus, Gauge parameter dependence and gauge invariance in the Abelian Higgs model, *Z. Phys. C* **75**, 739 (1997).
- [64] N. K. Nielsen, On the gauge dependence of spontaneous symmetry breaking in gauge theories, *Nucl. Phys.* **B101**, 173 (1975).
- [65] O. Piguet and K. Sibold, Gauge independence in ordinary Yang-Mills theories, *Nucl. Phys.* **B253**, 517 (1985).
- [66] P. Gambino and P. A. Grassi, The Nielsen identities of the SM and the definition of mass, *Phys. Rev. D* **62**, 076002 (2000).
- [67] S. P. Martin, Pole mass of the W boson at two-loop order in the pure $\overline{\text{MS}}$ scheme, *Phys. Rev. D* **91**, 114003 (2015).
- [68] S. P. Martin, Z-boson pole mass at two-loop order in the pure $\overline{\text{MS}}$ scheme, *Phys. Rev. D* **92**, 014026 (2015).
- [69] C. Becchi, A. Rouet, and R. Stora, The Abelian Higgs-Kibble model. Unitarity of the S operator, *Phys. Lett.* **52B**, 344 (1974).
- [70] G. Passarino and M. J. G. Veltman, One loop corrections for $e^+ e^-$ annihilation into $\mu^+ \mu^-$ in the Weinberg model, *Nucl. Phys.* **B160**, 151 (1979).
- [71] R. Oehme, On superconvergence relations in quantum chromodynamics, *Phys. Lett. B* **252**, 641 (1990).
- [72] R. Alkofer and L. von Smekal, The infrared behavior of QCD Green's functions: Confinement dynamical symmetry breaking, and hadrons as relativistic bound states, *Phys. Rep.* **353**, 281 (2001).
- [73] G. Curci and R. Ferrari, Slavnov transformations and supersymmetry, *Phys. Lett.* **63B**, 91 (1976).
- [74] D. Binosi and J. Papavassiliou, Pinch technique: Theory and applications, *Phys. Rep.* **479**, 1 (2009).
- [75] P. A. Grassi, B. A. Kniehl, and A. Sirlin, Width and partial widths of unstable particles, *Phys. Rev. Lett.* **86**, 389 (2001).
- [76] P. A. Grassi, B. A. Kniehl, and A. Sirlin, Width and partial widths of unstable particles in the light of the Nielsen identities, *Phys. Rev. D* **65**, 085001 (2002).
- [77] A. Maas, R. Sondenheimer, and P. Torek, On the observable spectrum of theories with a Brout-Englert-Higgs effect, *Ann. Phys. (Amsterdam)* **402**, 18 (2019).
- [78] A. Maas, Brout-Englert-Higgs physics: From foundations to phenomenology, [arXiv:1712.04721](https://arxiv.org/abs/1712.04721).
- [79] J. Frohlich, G. Morchio, and F. Strocchi, Higgs phenomenon without a symmetry breaking order parameter, *Phys. Lett.* **97B**, 249 (1980).
- [80] J. Frohlich, G. Morchio, and F. Strocchi, Higgs phenomenon without symmetry breaking order parameter, *Nucl. Phys.* **B190**, 553 (1981).
- [81] H. Sanchis-Alepuz, C. S. Fischer, C. Kellermann, and L. von Smekal, Glueballs from the Bethe-Salpeter equation, *Phys. Rev. D* **92**, 034001 (2015).
- [82] E. H. Fradkin and S. H. Shenker, Phase Diagrams of Lattice Gauge Theories with Higgs Fields, *Phys. Rev. D* **19**, 3682 (1979).
- [83] W. Caudy and J. Greensite, On the ambiguity of spontaneously broken gauge symmetry, *Phys. Rev. D* **78**, 025018 (2008).
- [84] A. Maas and T. Mufti, Two- and three-point functions in Landau gauge Yang-Mills-Higgs theory, *J. High Energy Phys.* **04** (2014) 006.